



# **Multimodal Microscopy of Focal Adhesions**

**Karin Legerstee**



# Multimodal Microscopy of Focal Adhesions

Karin Legerstee



# Multimodal Microscopy of Focal Adhesions

Multimodale microscopie van focal adhesions

**proefschrift**

ter verkrijging van de graad van doctor aan de  
Erasmus Universiteit Rotterdam  
op gezag van de rector magnificus

Prof. dr. R.C.M.E. Engels

en volgens besluit van het College voor Promoties.

De openbare verdediging zal plaatsvinden op  
dinsdag 29 september 2020 om 15.30 uur.

door

**Karin Legerstee**  
geboren te Utrecht

## **Promotiecommissie**

**Promotor:** Prof. dr. A.B. Houtsmuller

**Overige leden:** Prof. dr. N.J. Galjart  
Prof. dr. A. Cambi  
Prof. dr. L.F.A. Wessels

**Copromotor:** dr. W.A. van Cappellen







# Table of contents

	Scope of this thesis	8
<b>Chapter 1</b>	General introduction	
	A brief introduction to focal adhesions	12
	Multimodal microscopy of focal adhesions	21
<b>Chapter 2</b>	Dynamics of paxillin, vinculin, zyxin and VASP depend on focal adhesion location and orientation	41
<b>Chapter 3</b>	A novel photoconversion assay reveals foci of stably bound proteins within focal adhesions	67
<b>Chapter 4</b>	Growth factor dependent changes in nanoscale architecture of focal adhesions	91
<b>Chapter 5</b>	Correlative light and electron microscopy reveals fork-shaped structures at actin entry sites of focal adhesions	115
<b>Appendix</b>	Summary	132
	Samenvatting	134
	Scientific publications	137
	Curriculum Vitae	138
	PhD portfolio	140
	Dankwoord	142

# Scope of this thesis

The aim of the research described in this thesis is to increase knowledge of the structure and behaviour of focal adhesions and focal adhesion proteins through the application of a range of advanced light microscopy techniques. To increase the level of complementariness of the information gained from the different techniques, cell type (U2OS bone cancer cells) and ECM coating (collagen type I) were kept consistent in the research presented in this thesis. Additionally, focal adhesions in U2OS cells were consistently monitored by expressing one or two fluorescently tagged proteins selected from four hallmark focal adhesion proteins, paxillin, vinculin, zyxin and VASP. These proteins form functionally related pairs. Paxillin and vinculin are both large scaffold proteins while zyxin and VASP are both closely linked to the actin associated with focal adhesions.

**Chapter 1** provides a general introduction to focal adhesions, including their importance in health and disease and to cell migration in vitro and in vivo. This is followed by an overview of their molecular composition with special emphasis on paxillin, vinculin, zyxin and VASP. Additionally, advanced light microscopy techniques are introduced, with a focus on those applied in this thesis

In **chapter 2** we used total internal reflection (TIRF) microscopy in combination with Fluorescence Recovery After Photobleaching (FRAP) to examine and quantify the binding dynamics of the four selected focal adhesion proteins. We show that the stably bound fraction of paxillin and vinculin is surprisingly large and consistent across two different cell types from different species. Of the paxillin and vinculin proteins associated with focal adhesions, nearly half remains stably associated for times comparable to the average focal adhesion lifetime. Zyxin and VASP predominantly displayed more transient interactions. We also reveal a connection between focal adhesion protein binding dynamics and focal adhesion location and orientation, a connection which is particularly strong for zyxin and VASP.

In **chapter 3** we present a dedicated photoconversion assay using a FRAP set-up on a confocal microscope. Traditional FRAP can provide accurate estimates of the size of the stably bound fraction, the novel assay is used to specifically visualise the proteins of this fraction within a macromolecular complex, distinguishing it from its dynamically exchanging counterpart. We applied this assay to further investigate the particularly large stably bound fractions of paxillin and vinculin as seen in the FRAP experiments described in chapter 2. The assay revealed that the stably bound fractions of paxillin and vinculin form small clusters within focal adhesions. These clusters were predominantly observed at the half of the adhesion pointing towards the centre of the cell. Furthermore, the paxillin clus-

ters were markedly smaller than the vinculin clusters. This means the paxillin clusters are more concentrated than the vinculin clusters since the photobleaching data showed their stably bound fractions are of nearly equal size. Although in this thesis the developed technique was applied to focal adhesions, it can easily be applied to many different macromolecular complexes to specifically visualise the stably bound proteins within them.

In **chapter 4** we applied structured illumination microscopy to examine the distribution of paxillin, vinculin, zyxin and VASP along focal adhesions at superresolution level. We show that at the focal adhesion ends pointing towards the adherent membrane edge (heads), paxillin protrudes slightly further than the other proteins. At the opposite adhesion ends (tails) the other three proteins protrude further than paxillin, while at tail tips vinculin extended further than any of the other proteins. We also show scattering, which increases the random migration of cells, alters head and tail compositions. Furthermore, focal adhesions at protruding or retracting membrane edges had longer paxillin heads than focal adhesions at static edges.

In **chapter 5** we examine focal adhesions at an even higher resolution by using correlative light and electron microscopy, an imaging technique combining light microscopy with electron microscopy. We discovered a highly abundant distinct nanostructure around the actin fibre entry side formed by an area with increased protein density and possibly also with increased phosphorylation levels. In nearly three-quarters of focal adhesions, these nanostructures had a fork shape, with the actin forming the stem and the high density nanostructure within the focal adhesion the fork.

In conclusion, in this thesis a coherent set of experiments is described in which multiple advanced light microscopy methods and image analysis protocols were applied to increase insight in the dynamic composition of focal adhesions. This multimodal approach was chosen because each of the applied microscopy techniques has its own set of advantages and disadvantages. For this reason, the information gained was often complementary and sometimes synergistic, especially when the data was analysed quantitatively. A good example of this is that by combining the data described in chapters two and three, we were able to conclude that stably bound paxillin patches are more concentrated than stably bound vinculin. We also showed that the location and orientation of focal adhesions correlate with the dynamics of their intracellular proteins. Furthermore, the data described in the different chapters highlight that focal adhesions are non-uniform structures with two distinct tips which differ from each other in many aspects including in their protein dynamics, composition and density.



# Chapter 1

General introduction

## A brief introduction to focal adhesions

In their simplest form, eukaryotic cells are sacs of plasma membrane filled with cytoplasm, with a second set of membranes surrounding their DNA, the nucleus. Proteins are present throughout cells and form the majority of the cellular machinery. Structural support is provided by what is collectively termed the cytoskeleton, long filamentous proteins forming a network within the cytoplasm. In multicellular organisms, multiple cells group together in an organised fashion to form tissue. The extracellular matrix (ECM), a large three-dimensional macromolecular network surrounding the cells, adds further structure to the tissue. To maintain tissue integrity it is important that most cells remain fixed in place. For this purpose cells adhere both to each other as well as to the ECM.

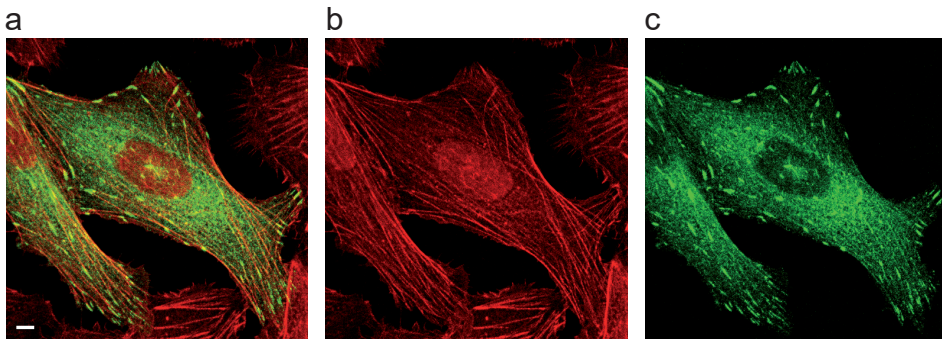


**Figure 1. Focal adhesions and F-actin stress fibres.**

(a) Overlay of the maximum projection of the confocal image of a U2OS cell stably expressing the intracellular FA protein paxillin-GFP (green) and stained with phalloidin-CF405 (pseudocolour red), a toxin that specifically binds to F-actin such as the stress fibres connecting to focal adhesions. Scale bar: 5  $\mu\text{m}$  (b) Pseudo coloured red channel of the data shown in a. (c) Green channel of the data shown in a.

Cellular adhesion to the ECM is facilitated by focal adhesions (FAs), flat elongated structures 1-5  $\mu\text{m}$  long, 300-500 nm wide and up to 50 nm thick<sup>1-4</sup> (Fig. 1a). They are macromolecular multiprotein assemblies that link the intracellular cytoskeleton to the extracellular matrix. Their linkage to the ECM is mainly mediated by integrins, transmembrane receptors that are part of the FA complex and directly bind to the ECM. Connection to the cytoskeleton takes place through stress-fibres, a specialised form of F-actin or filamentous actin, associated with contractile myosin II<sup>5</sup> (Fig. 1b). As protein complexes linking two constantly remodelling networks, the ECM and the cytoskeleton, FAs are continuously exposed to force. The force experienced by FAs depends on the combination of myosin-II contractility, which determines the force exerted on the FA by the stress fibres, and on the stiffness of the ECM. FAs are the points of force transmission from the cytoskeleton to the ECM and they change in number, size and

composition in response to the level of force experienced<sup>6-14</sup>.

### **Focal adhesions in health and disease**

Because of their importance in cell adhesion and for the transmission of force, FAs are crucial to most types of cell migration, including in vitro over a two-dimensional surface<sup>15</sup>. Since cell migration and adhesion are important in many physiological processes, FAs also play major roles in many physiological processes. Of note, FAs are vital to embryonic development, where they coordinate stem cell differentiation in response to ECM stiffness and are key to organogenesis and morphogenesis<sup>16-18</sup>. The importance of FAs is not limited to foetal physiological processes however, they are also pivotal to the normal functioning of the immune system and to wound healing<sup>19</sup>. Considering their importance to embryonic development and the immune system, it is unsurprising that FAs also have major roles in many developmental and immunological disorders<sup>15,18,19</sup>. Nevertheless, in pathology most FA research focusses on their role in cancer, where they are especially important during metastasis<sup>20-22</sup>. Integrins and other FA components are often upregulated in aggressive forms of cancer<sup>23-25</sup> and they are crucial to the Epithelial-Mesenchymal Transition (EMT)<sup>26-30</sup>. EMT is the process whereby epithelial cells, specialised cells that are arranged in layers and form most organs and tissue types, become more like mesenchymal cells, the less specialised typically highly motile cells that include stem cells and blood cells<sup>31</sup>. During EMT cells lose their cell-cell junctions, their dependency on cell adhesion and their apical-basal polarity. Cells also reorganise their cytoskeleton and activate different signalling and gene expression pathways during this process. Ultimately, EMT increases the motility and invasiveness of cells and therefore EMT is also an important step in tumour progression.

### **Focal adhesions on glass and in vivo**

FAs are large macromolecular multiprotein assemblies that vary in their overall structure and protein composition and to which differences in posttranslational modifications add further complexity<sup>32-34</sup>. The ECM is also complex, it is a large three-dimensional network with hundreds of different proteins, proteoglycans and glycosaminoglycans as possible components that is constantly being reorganised by matrix degrading enzymes<sup>35</sup>. There is also a direct interplay between the ECM and FAs, *i.e.* both ECM chemical composition and its mechanical properties (e.g. stiffness) influence FA composition, size and structure<sup>36,37</sup>. Because of the combined complexity of FAs, the ECM and their interactions, a coating of a single type of ECM protein on glass is often used for mechanistic studies. This strongly simplifies the complexity of the extracellular environment.

1

Although reducing complexity is a clear advantage for mechanistic studies, concerns have been raised about the relevance of FAs observed on coated coverslips to cell adherence and migration under physiological conditions. The primary concern is the extreme stiffness of glass (over 50 GPa) compared to the stiffness encountered in the human body, which ranges from ~1 kPa for the brain and ~10 kPa for muscle to ~100kPa for bones. Substrate stiffness has a direct impact on FAs and FA components. For example, if cells are cultured on glass or other stiff substrates the formed FAs are larger and expression of numerous FA proteins including talin, paxillin and vinculin is increased<sup>16,36</sup>. However, when cells are plated on gels with stiffness comparable to *in vivo* conditions, FAs are still observed. These FAs are composed of the same elements as FAs formed on glass, although they are typically smaller. A second concern is that glass coated coverslips provide a two-dimensional environment for the cells to bind to, instead of the three-dimensional ECM typically encountered *in vivo*. Again, this concern has been addressed using gels. In three-dimensional gels FAs are observed, which are smaller than FAs formed on glass but composed of the same proteins<sup>32,38</sup>. Therefore, FAs are not artefacts only formed when cells are exposed to very stiff two-dimensional environments. Indeed, FAs have been observed *in vivo* and recent *in vivo* studies confirmed their importance for several developmental processes and wound healing<sup>39-43</sup>.

### The molecular composition of focal adhesions

FAs were first described more than 40 years ago in reports that visualised the movement of cells on ECM-coated coverslips using interference reflection microscopy<sup>44-46</sup>. A decade later vinculin was the first intracellular FA protein described<sup>47,48</sup>. Since then, it has become apparent that FAs are large and diverse macromolecular protein assemblies, with over two hundred different reported proteins<sup>15,49</sup>. These include (trans)membrane receptors, adaptor proteins and many different signalling proteins such as kinases, phosphatases and G-protein regulators, which through post-translational modifications add significantly to FA complexity. Moreover, currently, a few thousand more proteins are candidates to be added to this list based on mass spectrometry experiments<sup>50,51</sup>. Intracellular FA proteins are organised in a layered nanostructure. A seminal study revealed the presence of three different layers: at the bottom, closest to the adherent membrane (within ~10-20 nm), the so-called integrin signalling layer (ISL), at the top (~50-60 nm from the adherent membrane) the actin-regulatory layer (ARL) and in between the force transduction layer (FTL)<sup>3</sup>. Later studies, using different techniques, confirmed the layered nanostructure of FAs along the z-axis<sup>52-54</sup>.



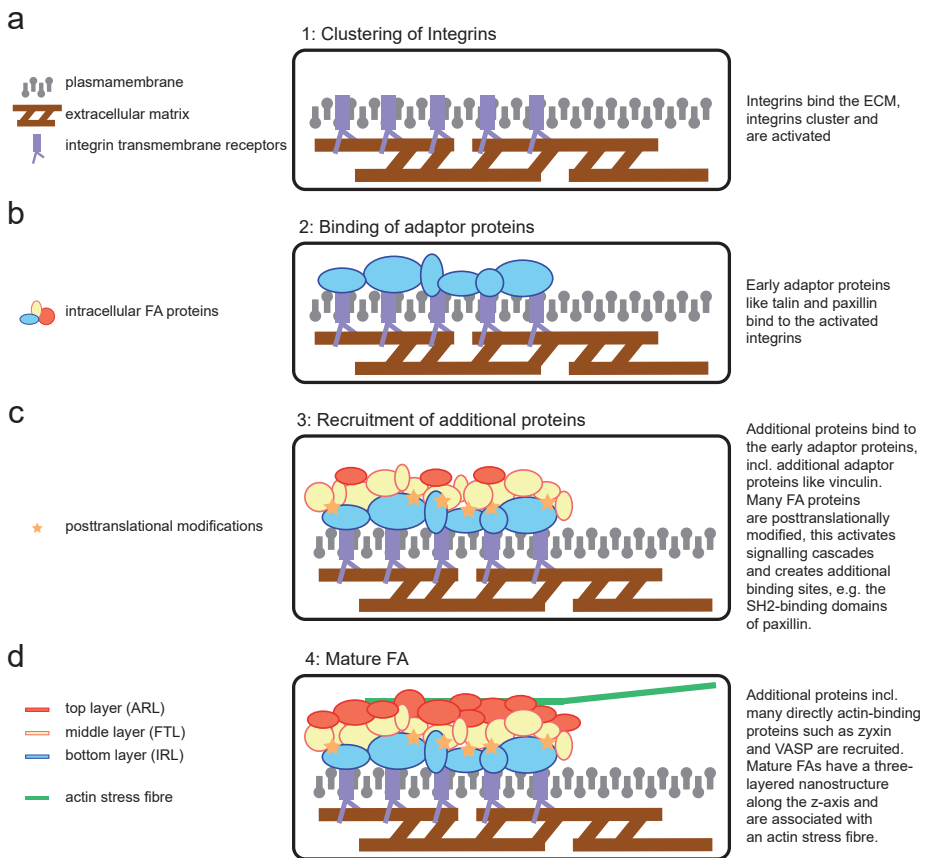


**Figure 2. The formation of a focal adhesion complex through time.**

(a-d) Simplified overview of the main steps involved in the formation of a focal adhesion complex. Steps shown in chronological order, from the initial clustering of integrin receptors (a) to the eventual formation of a mature three-layered focal adhesion with associated F-actin stress fibre (d). Not to scale.

The characteristics of individual FAs, including their molecular composition, varies greatly depending on the different inputs they receive from their local environments, both intracellularly and from the ECM. However, all FAs incorporate integrin transmembrane receptors and actin stress fibres. Integrins are heterodimers of  $\alpha$ - and  $\beta$ -integrins, in mammalian cells 24 different heterodimers have been reported, all with their own ligand specificity for (sets of) ECM proteins<sup>55</sup>. There are two types of stress fibres associated with FAs: ventral stress fibres are associated with FAs at either end and typically transverse the whole cell<sup>56</sup>. Dorsal stress fibres are linked to FAs on one end, typically near the cell front, then stretch upwards to the nucleus and the dorsal cell surface.

The formation of new FA complexes involves several steps (Fig. 2). Firstly, in-

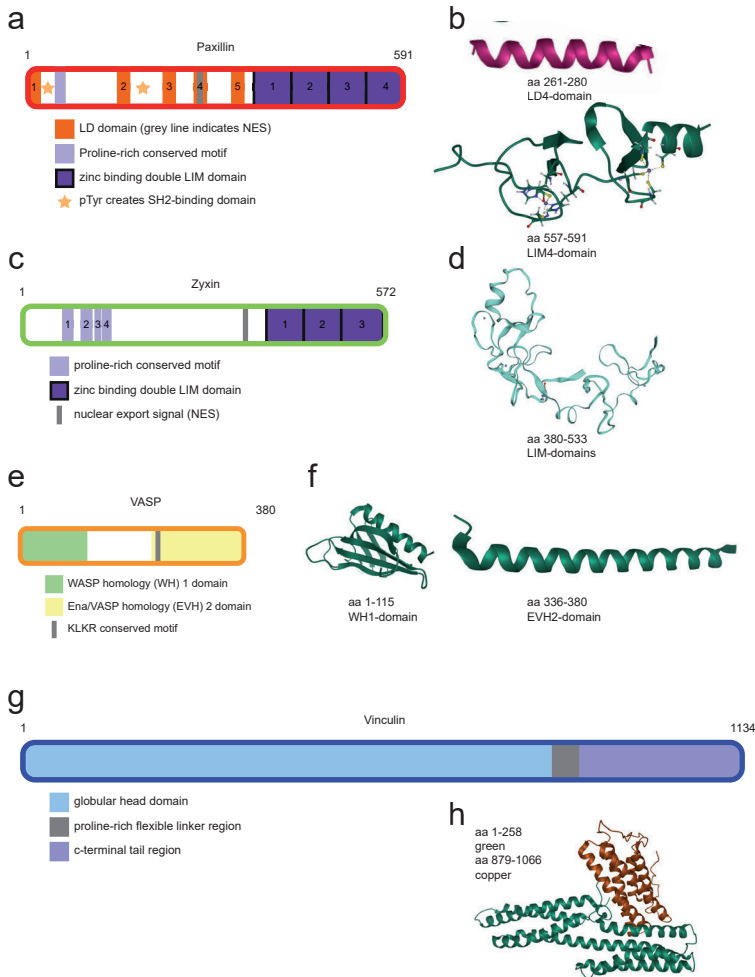


**Figure 3. The structure of four intracellular FA proteins.**

(a, c, e, g) Schematic representation of the paxillin (a), zyxin (c), VASP (e) and vinculin (g) proteins and their different domains, drawn to scale with respect to the amino acid backbone. Numbers indicate amino acid number along the protein backbone. (b) 3D structures of paxillin domains as visualised using the RCSB ProteinDataBank structure viewer Mol<sup>®</sup>169. Top: 3D structure of the LD-4 domain, which includes the paxillin nuclear export signal (NES). Based on X-ray diffraction data PDB ID: 6IUI<sup>170</sup>. Bottom: 3D structure of a large part of the paxillin LIM 4 domain based on Nuclear Magnetic Resonance (NMR) spectroscopy data PDB ID: 6U4M<sup>171</sup>. The blue spheres represent the two bound zinc-ions, amino acids interacting with these ions are visualised using the 'ball and stick' method. (d) Predicted 3D structure of a stretch spanning part of the first and all of the second and third zyxin LIM domains as predicted by the SWISS-MODEL database based on its homology with the LIM domains of the insulin gene enhancer protein ISL-2 with known 3D structure through X-ray diffraction data<sup>172,173</sup>. (f) 3D structures of VASP domains. Left: WH1-domain based on NMR spectroscopy data, PDB ID: 1EGX<sup>174</sup>. Right: structure of the last part (termed block C) of the EVH2-domain based on X-ray diffraction data, PDB ID: 1USE<sup>175</sup>. (h) 3D structure of the parts of the vinculin head and tail domains in complex when vinculin is in its closed conformation. Based on X-ray diffraction data, PDB ID: 1RKE<sup>176</sup>.

tegrin transmembrane receptors bind to the extracellular matrix, which causes clustering of the integrins, leading to their activation with resultant conformational changes<sup>8,57-59</sup> (Fig. 2a). Secondly, intracellular adaptor proteins such as talin and paxillin are recruited<sup>60,61</sup> (Fig. 2b). These proteins in turn promote integrin activation, leading to the clustering of more integrins<sup>62</sup>. The adaptor proteins also provide a binding platform for the hundreds of other intracellular FA proteins which ultimately results in the recruitment of an actin stress fibre (Fig. 2c,d).

### *Paxillin*

As an adaptor protein, paxillin is one of the proteins with the largest number of potential binding partners within FAs<sup>49</sup>. Paxillin is a direct integrin-binding protein present in the bottom (IRL) layer and it is among the first proteins to be recruited to newly forming FAs<sup>3,60,61</sup> (Fig. 2b).

The N-terminal domain of paxillin has two binding sites for Focal Adhesion Kinase (FAK), which can phosphorylate paxillin at Tyr-31 and Tyr-118<sup>63,64</sup> (Fig. 3a). This phosphorylation creates two SH2 binding sites, which are the main binding platforms for the other paxillin interactors, among which are many signalling proteins such as the kinase Src<sup>65</sup>. The phosphorylation process is mechanosensitive, *i.e.* it depends on the level of force experienced by the FA, where in this case, force increases phosphorylation levels<sup>14</sup>. Unsurprisingly, the creation of the SH2 binding domains through tyrosine phosphorylation of paxillin, is a key step during FA assembly<sup>66</sup>. It influences FA size, can be used as a measure of integrin signalling and is increased during EMT induced by transforming growth factor  $\beta$  (TGF- $\beta$ ) in various cell lines<sup>29,30,67,68</sup>. Incidentally, zyxin is required for efficient tyrosine phosphorylation of paxillin during TGF- $\beta$ -induced EMT.

The C-terminal domain of paxillin contains four double zinc finger LIM domains, reminiscent of zinc finger transcription factors<sup>64</sup> (Fig. 2a,b). Indeed, paxillin is a functioning transcription factor, has a nuclear export signal and shuttles between FAs and the nucleus<sup>69,70</sup>. Furthermore, paxillin influences gene expression at the translational level by interacting with polyadenylate-binding protein 1 (PABP1), both at the endoplasmic reticulum and at FAs<sup>71,72</sup>. Aside from their critical role in transcription regulation the paxillin LIM domains are also required for its targeting to FAs, in particular the third LIM domain<sup>64</sup>.

Consistent with paxillin being a key adaptor protein for FAs, paxillin knockout mice suffer from lethal heart and brain deficits during embryonic development<sup>73</sup>. Fibroblasts cultured from paxillin knockout mice display aberrant FAs, decreased migration and problems with cell spreading. This highlights the importance of paxillin to FAs and by extension to cell adherence and migration.

## Zyxin and VASP

1 Zyxin and vasodilator-stimulated phosphoprotein (VASP) are binding partners that are recruited together to forming FA complexes at relatively late stages<sup>74-76</sup> (Fig. 2d). They are closely linked to the stress fibres associated with mature FAs and are found in the top (ARL) layer<sup>3</sup>. They accumulate at FAs and at actin-polymerisation complexes, which are periodically distributed along stress fibres<sup>77-79</sup>. Zyxin recruits VASP and  $\alpha$ -actin to damaged stress fibres to coordinate their repair and maintenance<sup>80</sup>. VASP is part of the Ena/VASP protein family, a group of highly related proteins named for the drosophila protein enabled and its vertebrate homologue VASP.

The C-terminal domain of zyxin contains several double zinc finger LIM domains<sup>81</sup> (Fig. 3c,d). Zyxin is a functioning transcription factor, has a nuclear export signal and moves, particularly in response to force, from FAs to the nucleus where it promotes gene expression<sup>69,82,83</sup>. Nuclear zyxin is involved in the control of mitosis progression<sup>79</sup>. Since it is a direct polyadenylate-binding protein zyxin can influence protein expression at the translational level, next to its role at the transcriptional level<sup>84</sup>. Finally, the zyxin LIM-domains are responsible for its targeting to FAs, where zyxin is responsible for the mechanosensitive recruitment of VASP<sup>75,85,86</sup>. Note that this is similar to the role of the LIM domains in paxillin function.

The zyxin N-terminus is closely linked to actin regulation. It contains actin binding sites, but also binding sites for  $\alpha$ -actinin, an actin-binding protein that is especially abundant on stress fibers<sup>87,88</sup>. Proline-rich stretches form binding sites for the Ena/VASP proteins<sup>75,76</sup> (Fig. 3c). These stretches are also binding sites for guanine exchange factors (GEFs) for the small GTPase Rho, through which zyxin, VASP and vinculin, in a co-dependent manner, stimulate actin polymerisation in response to mechanical stimuli<sup>75,85,89-93</sup>.

In mammals the Ena/VASP family consist of three different proteins: VASP, mammalian protein enabled homolog (Mena) and Ena-VASP-like protein (Evl). These proteins are highly related and share the same functional domains (Fig. 3e). The N-terminus incorporates the WASP homology (WH) 1 domain, also known as the Ena/VASP homology (EVH) 1 domain (Fig. 3f). This is a protein interactor domain which binds to a specific proline-rich motif such as is present in zyxin and vinculin<sup>94</sup>. As discussed above, zyxin recruits VASP to FAs and consequently the WH 1 domain is also essential for the targeting of VASP to FAs.

The C-terminus of the Ena/VASP proteins contains the EVH 2 domain, which is closely linked to their actin regulatory functions (Fig. 3e). The EVH2 domain is

composed of three consecutive regions termed blocks A, B and C. The conserved KLKR motif within block A mediates the stimulation of actin polymerisation. Block B contains an F-actin binding site and block C terminates in a large alpha-helix (Fig. 3f). This alpha-helix mediates the tetramerization of the Ena/VASP proteins, which is required for their efficient functioning<sup>95</sup>.

The study of VASP depleted or VASP knockout cells or mice is hampered by the presence of the other Ena/VASP family members. Nevertheless, a recent study using somatic gene disruptions of all three family members showed the Ena/VASP proteins positively contribute to cell adhesion and cell migration over two-dimensional stiff surfaces<sup>96</sup>. Zyxin knockout mice display no lethal embryological developmental problems or obvious histological abnormalities<sup>69,97</sup>. However, loss of zyxin, VASP or their interaction, results in an inability of cells to remodel their cytoskeleton in response to internal or external cues. Such cells are no longer able to thicken their stress fibres in response to mechanical stress or the actin stabilizer jasplakinolide<sup>89,90,98</sup>. This translates into an inflexibility of cellular behaviour. Fibroblasts cultured from zyxin knockout mice are unable to adjust their migratory speed or adhesiveness in response to cues from the ECM, although overall both migration and adhesiveness are enhanced in these cells compared to wild type.

The upregulation of zyxin is also a part of the TGF- $\beta$  induced EMT response, where zyxin coordinates the remodelling of the actin cytoskeleton during EMT<sup>29</sup>. In line with this important role of zyxin in the EMT process, zyxin has been strongly linked to several types of cancer (progression), including bladder and breast cancer and Ewing's sarcoma where it acts as a tumour suppressor<sup>99-101</sup>.

### *Vinculin*

Vinculin is a large scaffold protein similar to paxillin and it is among the proteins with the most potential interaction partners within FAs<sup>49</sup>. Vinculin is among the earliest proteins recruited to newly forming FAs, although vinculin does not directly bind to the clustering integrins and consequently is recruited slightly later than paxillin<sup>49,74</sup> (Fig. 2c). Vinculin directly binds actin filaments and is involved in actin regulation at FAs<sup>102</sup>. It is found in the middle (FTL) layer of mature FAs<sup>3</sup>.

Vinculin has a head and a tail domain with a flexible linker in between, allowing vinculin to adopt open and closed conformations<sup>103</sup> (Fig. 3g). In its closed, or inactive form, the head and tail domain interact (Fig. 3h). When vinculin opens to its active form several extra protein binding sites are revealed.

The vinculin head domain shares many important binding partners with paxillin, including talin<sup>104</sup>. Together with paxillin and talin, vinculin promotes integrin

1

activation and clustering<sup>102</sup>. The head domain also has a binding site for paxillin and paxillin is required for vinculin's recruitment to FAs in many, but not all, cell types<sup>14,64,73,105,106</sup>. This process is particularly well-studied in fibroblasts, where the paxillin-mediated recruitment of vinculin is force-dependent and as such is affected by both myosin-II contractility and matrix stiffness<sup>14</sup>. It requires tyrosine phosphorylation of paxillin, which is mediated by FAK in a mechanosensitive manner. The interaction between vinculin and paxillin also inhibits the translocation of paxillin to the nucleus<sup>107</sup>.

The vinculin tail domain is closely linked to actin regulation. It contains actin binding sites but also binding sites for  $\alpha$ -actinin and the Ena/VASP proteins<sup>108-111</sup>. Vinculin requires both zyxin and VASP to efficiently stimulate actin polymerisation at FAs<sup>75,89-93</sup>.

Vinculin knockout mice, like the paxillin knockout mice, experience lethal heart and brain deficits during embryonic development<sup>112</sup>. Induced vinculin 'knockout' embryonic fibroblasts display problems with cell spreading, with adhesion to a variety of different substrates, with three-dimensional invasion, with FA maturation and with forming strong traction forces at FAs, although their random migration velocity is increased<sup>113-116</sup>. This shows that as another large adaptor protein vinculin, like paxillin, is of great importance to FAs and by extension to embryonic development.

### The scattering response

A considerable part of the FA research field focuses on studying FAs during cell migration, mainly because of the importance of cell migration to embryonic development and metastasis. An often employed method to enhance cell migration is to stimulate cells with the Hepatocyte Growth Factor (HGF). HGF, also known as the scattering factor, induces a scattering response in epithelial cells<sup>117-120</sup>. During scattering the contact between cells is reduced and cells display increased motility and undirected migration.

#### *The hepatocyte growth factor (HGF) and Met*

HGF is an 80 kDa protein that was first discovered as the natural ligand for the tyrosine receptor encoded for by the proto-oncogene c-Met<sup>121-123</sup>. Both HGF and Met are glycosylated and cleaved by proteases from single-chain precursors into mature disulphide-linked heterodimers<sup>124</sup>. HGF is the only known natural ligand for Met and Met is the only known receptor for HGF. Upon HGF binding the kinase activity of Met is activated through autophosphorylation. Further phosphorylation creates docking sites for different intracellular signalling molecules that activate a host of signalling pathways with diverse biological effects<sup>117</sup>.

### *HGF in health and disease*

HGF/c-Met signalling is indispensable for organogenesis<sup>125</sup>, during adulthood it is involved in the response to damage and in the maintenance of homeostasis of several organs<sup>126</sup>. In pathology, HGF signalling through c-Met is involved in the progression of several infectious diseases, but it is probably best known for its involvement in cancer, in particular for its promotion of metastasis<sup>118,127-129</sup>. As such, HGF/Met signalling is considered a promising target for the treatment of different cancer types<sup>127,128,130-132</sup>. The aberrant HGF/Met signalling seen in cancer (1) stimulates angiogenesis, (2) promotes survival of cells after detachment from the basal membrane by inhibiting apoptosis through a wide variety of mechanisms, (3) stimulates the excretion of proteases to allow cells to invade through the ECM and (4) strongly stimulates cell motility<sup>127,128,133,134</sup>. Taken together this explains the important role of HGF in metastasis.

## Multimodal imaging of focal adhesions

Over the last few decades, the field of biology has greatly benefited from the development of different advanced light microscopy techniques. At their basis lie two important technological advances, the use of lasers as a light source and the development of genetically encoded fluorescent tags.

### **Lasers as a light source**

Probably the most well-known microscopy form using lasers as a light source is confocal laser scanning microscopy<sup>135,136</sup>. This form of microscopy uses a laser to scan samples and pinholes to block out of focus light, which greatly improves image quality. Even without pinholes lasers offer significant improvements to light microscopy because of their ability to exclusively produce coherent light of a specific wavelength and because they are such powerful light sources, with more powerful lasers being developed all the time.

### **GFP and other genetically encoded fluorescent tags**

Green Fluorescent Protein (GFP) is a small 27 kDa protein that was first isolated from the *Aequorea victoria* jellyfish in the sixties<sup>137</sup>. GFP became of key importance to cell biology with the realisation that it could be used to tag and follow proteins in live cells<sup>138</sup>. For this purpose, cells are transfected with engineered DNA constructs, in which the DNA encoding for GFP is added to the DNA encoding a protein of interest. As a result, fusion proteins of the protein of interest fused to GFP are produced by the DNA transcription machinery of the transfected cells. The GFP effectively functions as a 'build-in light' that turns on when it is excited by light of the appropriate wavelength, allowing the protein to be followed in

1 live cells. Since the first genetically encoded fluorescent tags, much research has led to the development of a significantly improved toolset. Brighter proteins are now available with emission wavelengths that span the entire colour spectrum and even beyond it into the ultraviolet and far-red wavelengths. The different colours do more than just create pretty images, they allow the visualisation of different fusion proteins at the same time because they can be distinguished through their colours.

### **Imaging fluorescent molecules**

When GFP or other fluorescent molecules absorb photons with a specific amount of energy, their electrons change configuration to bring the molecules from the ground state to an excited state. Because this state is energetically unfavourable, the electrons quickly fall back to the ground state. During this process, the electrons release their excess energy in the form of a photon, which is known as fluorescence. Some energy is always lost during excitation, therefore the photons emitted by fluorescent molecules always have less energy than the photons they need to absorb for excitation. Consequently, the light emitted by fluorescent molecules always has a longer wavelength than the light they need to absorb for excitation since the wavelength of light is determined by the energy level of its photons and less energy means a longer wavelength. The emitted light also has a much lower intensity, typically the light used for excitation is approximately a thousandfold stronger than the light emitted. So, to make a clear image of the emitted light it needs to be filtered from the excitation light. Because of the different wavelengths, in fluorescence microscopes this can easily be achieved using chromatic filters which filter light of specific wavelengths.

### **Advanced light microscopy in the field of biology**

The use of lasers as a light source and the development of genetically encoded tags opened up the road for the development of advanced light microscopy techniques and their application in the field of biology. As image quality improved with continuing development over time, light microscopy became one of the main research methods in cell biology. However, no matter how bright the lasers or how good the lenses, in principle the laws of physics place a limit on the resolution a light microscope can achieve. This was first recognised by the German scientist Ernst Karl Abbe (1840-1905) and is often referred to as Abbe's limit or simply the resolution limit. Ultimately, it means that the maximum resolution (the smallest distance at which two objects can still be resolved as being separate) a light microscope can ever achieve is approximately half the wavelength used for excitation. When using GFP this theoretical maximum resolution is approximately 250 nm. Since protein sizes range from about one to five nanometers, ide-



ally cells would be observed at considerably higher resolutions. Consequently, much of the modern advanced microscopy methods are focused on clever ways to break, or more accurately circumvent, the resolution limit. These include TIRF, SIM and single molecule imaging techniques such as PALM or STORM. Other advanced imaging techniques focus on using microscopy to obtain additional information from the images, information beyond the location of proteins. Examples of such techniques include FRAP, FCS and STICS, which focus on obtaining quantitative measurements related to the dynamic behaviour of proteins.

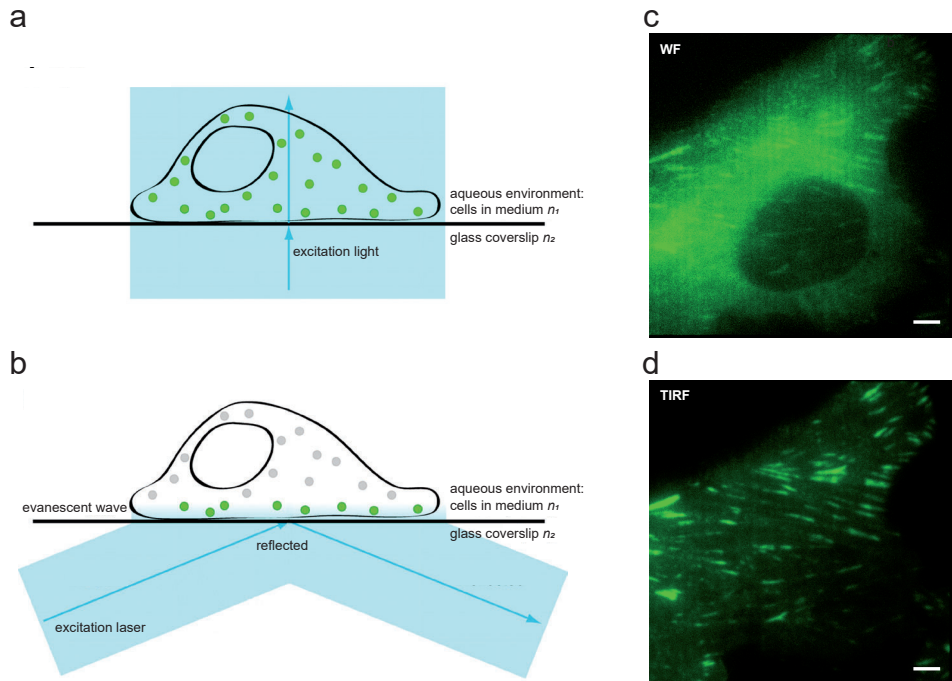


**Figure 4. Widefield versus total internal reflection microscopy.**

(a) Schematic overview of the light path during widefield or epifluorescence microscopy. The excitation laser shines straight through the sample, therefore fluorophores are excited throughout the cell (green circles). (b) Schematic overview of the light path during total internal reflection (TIRF) microscopy. The excitation laser exits the objective at such an angle that it is completely reflected at the glass-fluid interphase, formed by the glass coverslip and the aqueous environment of the cells in media, back into the objective. The reflecting laser light produces an electromagnetic field known as the evanescent wave, which declines exponentially. It is only powerful enough to excite fluorophores (green circles) in a thin layer 100-200 nm upwards from the coverslips, leaving fluorophores present at higher locations in the cell unexcited (grey circles). (c, d) The same area of a U2OS cell stably expressing paxillin-GFP imaged on the same microscope in widefield (c) or in TIRF (d) mode. In d the signal to background ratio is strongly improved for the focal adhesions.

#### *Total internal reflection microscopy*

Total internal reflection (TIRF) microscopy breaks the resolution limit in one direction by changing the angle of the excitation laser. It was first developed in the early eighties<sup>139</sup>, then adapted for easy use in cell biology in the late eighties<sup>140</sup>. In

1

TIRF the excitation laser illuminates the sample at an angle. Consequently, the laser is reflected at the glass-fluid interphase because of the difference in refraction index between the glass coverslip and the aqueous solution (the cytoplasm or the culture medium) on top (Fig. 4b). The angle is adjusted to the precise angle where the entire laser beam is fully reflected back into the objective. This is known as total internal reflection and it is the same principle as is used for data transfer through fibre-optic cables. As implied by the 'total', in TIRF microscopy the entire laser beam is reflected at the glass-fluid interphase and its light is not directly used to excite fluorophores. The reflecting laser light produces an electromagnetic field, the evanescent wave. Because the wave declines exponentially, it is only strong enough to excite fluorophores up to a very small distance from the glass-fluid interphase, about 100-200 nm. In other words, only a thin layer one to two hundred nanometres upwards from the coverslip is visualised, breaking the resolution limit in this direction.

The thinness of the excitation layer limits the cellular objects that can be studied with TIRF to those found in, or very close to, the plasma membrane. Despite this limiting effect, the thinness is also the reason for the main advantage of TIRF, the strongly improved signal to background ratio. Any fluorophores further than two hundred nanometers from the adherent plasma membrane are not reached by the evanescent wave, for this reason, they are not excited and the potential background fluorescence is eliminated. When visualising FAs by fluorescently tagging intracellular FA proteins this effect is especially pronounced because these proteins are typically strongly expressed in the cytoplasm apart from their enrichment at FAs, increasing the potential for background fluorescence coming from the cytoplasm (Fig. 4c,d). Other advantages of the thin excitation layer are that almost no out-of-focus fluorescence is collected, also improving image quality, and cells are exposed to relatively little light, reducing phototoxicity.

#### *Structured illumination microscopy*

Structured Illumination Microscopy (SIM) also uses a specialised form of illumination to improve resolution. While in TIRF only the z-resolution is improved, SIM circumvents the resolution limit in all three directions<sup>141</sup>. In each direction, the resolution is improved approximately two-fold compared to a confocal microscope, in essence enabling the visualisation of three-dimensional objects eight ( $2^3$ ) times as small<sup>142</sup>.

The specialised illumination in SIM makes use of a grating pattern of light, which produces the Moiré effect. This phenomenon is a type of interference that occurs when two dense patterns are overlaid and it produces a third, larger pattern (Fig. 5a). In SIM, images are reconstructed through a complicated mathematical pro-

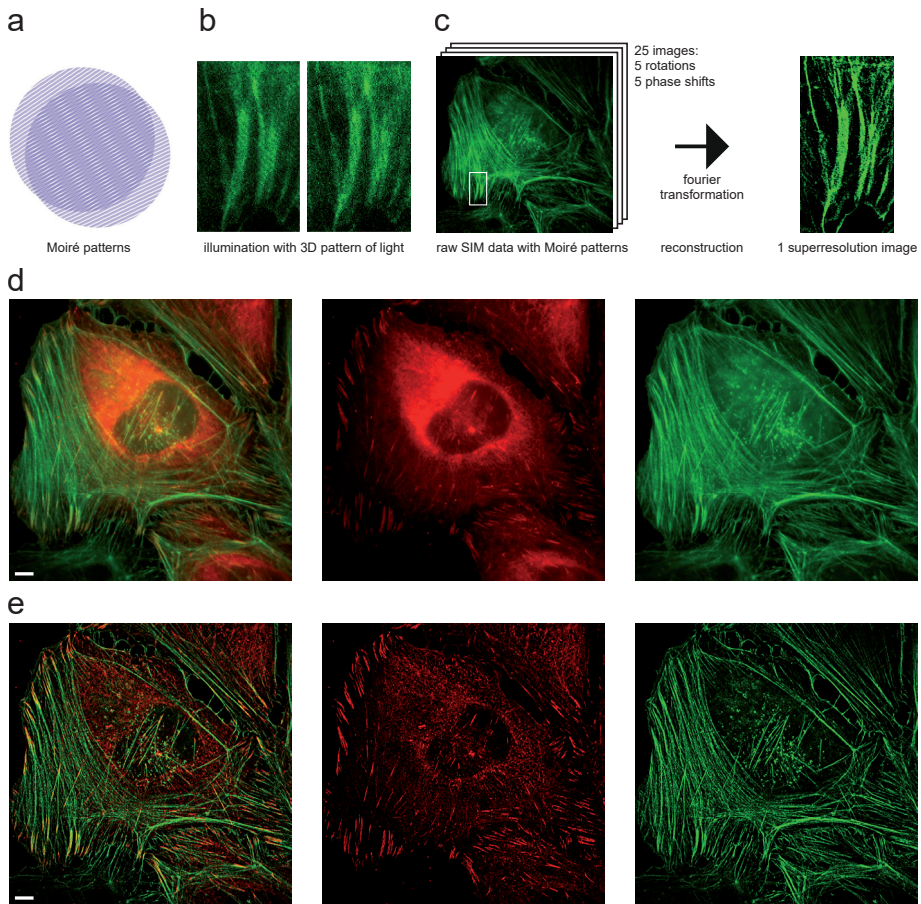


**Figure 5. Structured Illumination Microscopy (SIM)**

(a) Example of a Moiré pattern, an interference effect that occurs when two dense patterns are overlaid. Note that the formed Moiré pattern is always larger than the overlaid patterns. (b, c) An overview of SIM imaging. SIM uses a grating three dimensional pattern of light for illumination, meaning parts of the sample are not exposed to excitation light (black stripes in b). This form of illumination produces Moiré effects. Note that the black stripes in b change orientation, this is because the pattern of light is rotated to allow reliable reconstruction of the superresolution image based on the collected Moiré patterns (c). The illumination pattern is also shifted to allow data collection from the whole image. In total 25 raw data images are used to reconstruct 1 superresolution image. b is a magnification of the boxed area in c (d, e) Reconstruction of the widefield image (d) or the superresolution SIM image (e) of a U2OS cell stably expressing paxillin-mCherry (red) and stained with phalloidin-CF405 (pseudocolour green) to highlight the F-actin. Scalebar: 5  $\mu\text{m}$

cess involving Fourier transformations, on the basis of the (known) illumination pattern and the Moiré pattern observed in the raw data (Fig. 5b,c). This allows reconstruction of images beyond the resolution limit (Fig. 5e) because the Moiré patterns they are based on are always larger than the original overlaid patterns. In other words, in the Moiré patterns high frequency data is shifted to a lower, observable, frequency<sup>143</sup>. During the reconstruction process, this data is shifted

1 back to its high frequency position in Fourier space, then translated into a reconstructed high resolution image. To allow for reliable reconstruction the Moiré patterns need to be collected following 3 to 5 rotations of the illumination pattern. To make sure the whole image is covered by the illumination pattern it needs to be shifted as well. Accordingly, to create one reconstructed SIM image, 25 raw images need to be collected, slowing down the imaging process. Because SIM is a widefield technique, the whole image (or at least the whole image currently covered by the illumination pattern) is collected at once, hence SIM is still fast enough for live cell imaging despite the large number of raw images needed to reconstruct one superresolution image.

### *Correlative light and electron microscopy*

A different approach to achieving a higher resolution is to couple light microscopy with electron microscopy. Electron microscopy (EM) uses an electron beam for visualisation purposes. Electron beams have wavelengths about a hundred thousand times smaller than light beams<sup>142</sup>. This means that even resolutions sufficient to visualise single molecules can easily be achieved without approaching Abbe's limit.

EM does not necessarily rely on tags for visualisation, where in fluorescence microscopy (FM) only the fluorescently tagged protein is visible, in EM all are visualised at the same time. This reveals the cellular context, but also makes it difficult to recognise specific structures or individual protein types, such as are easily identified in FM by their fluorescent tags. This problem is largely solved in Correlative or Correlated Light and Electron Microscopy (CLEM), which as the name suggests combines the two imaging modalities of light (typically fluorescence) microscopy and electron microscopy<sup>144</sup>. This allows the visualisation of a specific protein type, recognisable through FM, at high resolution and within the cellular context through EM.

Different types of EM can be used in CLEM. Since focal adhesions are dense structures found close to the cell surface they are particularly well suited to studying with scanning EM. In this technique images are formed by collecting electrons scattered by the sample surface, limiting imaging to a thin layer close to the sample surface. Density influences this scattering, making the dense FA complexes stand out from their surrounding environment. Using scanning EM eliminates the need for the complicated sample preparation required for transmission EM and simplifies the combination with FM.

In some forms of CLEM the FM is performed first followed by EM sample preparation and EM imaging, in others sample preparation is completed first followed

by both FM and EM imaging<sup>145</sup>. This second approach can improve the quality of the FM and EM overlay images. Firstly by avoiding the risk of EM sample preparation leading to distortions between the FM and EM images. Secondly, by allowing for both types of imaging to be performed on a single microscope, which makes it much easier to ascertain the exact same structure is imaged in both modalities. This approach of combining FM and EM in a single microscope was first achieved in the eighties<sup>146</sup>. It is termed integrated CLEM and currently microscopes using this approach are commercially available<sup>145</sup>.

### *Fluorescence recovery after photobleaching*

Fluorescence Recovery After Photobleaching (FRAP) is one of the advanced light microscopy techniques not aiming to enhance the resolution but focusing on obtaining quantitative parameters, specifically on the mobility and dynamics of proteins. FRAP was initially conceptualised and set-up at the end of the seventies<sup>147-149</sup>. When around the beginning of the millennium both laser-assisted microscopy and genetically encoded fluorescent tags became widely available, the rapidly expanding field of protein dynamics embraced FRAP as one of its principal tools of investigation<sup>150-154</sup>.

FRAP takes advantage of the fact that when fluorescent tags are excited too strongly they irreversibly lose their fluorescent property, i.e. they are bleached. During a typical FRAP experiment, a small region of the cell is briefly illuminated with a powerful laser, bleaching the fluorescent tags of the fusion proteins exposed to this so-called bleach pulse. As a result, when this area of the cell is again illuminated by the excitation laser at its normal strength, the fluorescent light emitted is markedly reduced or even lost altogether. During a FRAP experiment, fluorescence levels are recorded and plotted against time in FRAP-curves. If the tagged proteins are able to move, over time the fluorescence levels will go up again, as the bleached proteins are replaced by fusion proteins with intact, unbleached, fluorescent tags moving into the bleached area.

From FRAP-curves a lot of information can be extracted about the mobility and binding dynamics of the studied proteins. For example, the steepness of the recovery curve is related to the mobility of the studied protein. The faster a protein moves the steeper the recovery of its FRAP-curve will be, since after the bleach pulse the unbleached molecules will move into the bleached area more quickly, resulting in a faster rise of fluorescence levels. If the final steady fluorescence level is much lower than the initial steady pre-bleach level, this reveals that a significant proportion of the proteins in the bleached area are stably bound and accordingly do not exchange for unbleached proteins within the time of the experiment. This means at the end of the experiment these bleached proteins are

still present within the bleached area, lowering the measured fluorescence levels. Of note, lower post-bleach fluorescence levels may also point to technical issues (such as monitor bleaching or bleaching of a too large proportion of the protein pool). These need to be ruled out through control experiments.

1 One of the key advantages of the FRAP technique is its swiftness: individual FRAP-experiments can often be conducted within a few minutes and neither the preparation nor the data analysis required to generate the FRAP-curves is particularly complicated or time consuming. This makes it especially well-suited to the extraction of reliable quantitative parameters by using the data from a high number of replicate experiments. Particularly if the experimentally-derived FRAP curves are further analysed by fitting them to curves generated by Monte Carlo based simulations<sup>155</sup>. This makes it possible to reliably extract from the FRAP curves many quantitative parameters, including the number of fractions with distinct dynamic parameters present within the protein pool, the sizes of these fractions and the associated  $k_{on}$ 's and  $k_{off}$ 's, while avoiding most of the simplification steps needed for the more traditional FRAP-curve analysis of mathematically solving differential equations<sup>147,156</sup>.

### *Photoactivation and photoswitching*

Besides brighter proteins with a diverse range of emission wavelengths, the continuing optimisation of fluorescent proteins also led to the development of proteins with altered emission characteristics in response to light of certain wavelengths, because of photochemical reactions or through conversions between chromophore stereoisomers<sup>157</sup>. These include the photoactivatable and the photoswitchable or photoconvertible fluorescent proteins<sup>158</sup>.

Photoactivatable proteins require activation by illumination at a wavelength shorter than their excitation wavelength to become efficiently fluorescent. One of the first developed was photoactivatable GFP, a variant of GFP which after illumination with its activation wavelength (413 nm) becomes a hundred times more fluorescent at the wavelengths normal for enhanced GFP<sup>159</sup>. Continuing development has led to the engineering of a large number of photoactivatable fluorescent proteins with differing characteristics, for example in the emission spectrum, in the brightness and in the reversibility of the activation<sup>160</sup>.

For the photoswitchable or photoconvertible fluorescent proteins irradiation with laser light of roughly four hundred nanometers results in a shift of their excitation and emission spectra. Again, continuing research has led to the development of a large number of photoconvertible fluorescent proteins together spanning a large emission spectrum with varying levels of brightness and revers-

ibility<sup>160</sup>. An example of a third generation optimised photoswitchable protein is mMaple3. It is a green fluorescent protein which after activation is converted to a red fluorescent protein. It is among the brightest and the most efficiently switched of the currently available photoswitchable proteins, yet it shows extremely low dimerization tendencies (a major concern for the other bright photoswitchable proteins)<sup>161</sup>.

A common application of photoswitchable and photoactivatable proteins is in the superresolution techniques Photo Activated Location Microscopy (PALM) and Stochastic Optical Reconstruction Microscopy (STORM)<sup>162-164</sup>. In these forms of single molecule microscopy, low light intensities are used for photoswitching or photoactivation, making these processes slow enough to allow individual switched or activated fluorescent proteins to be sequentially detected, which in turn allows their localisation with increased precision.

#### *Advances in data analysis*

Large improvements in the employed data analysis methods also contributed strongly to the increased importance of light microscopy to modern biology, next to all the technological advances involving the light microscopes and fluorophores. Most notably the single-molecule techniques of PALM and STORM depend entirely on post-acquisition data analysis techniques for the creation of their superresolution images. Raw PALM or STORM data resembles a long series of images with less than a hand full of activated or switched fluorophores in each separate image. Because of the optical limitations of the imaging system these fluorophores are imaged as larger spots than they actually are to form a diffraction-limited spot described by the point spread function. To generate superresolution images from this raw data extensive data analysis is required. Firstly, the point spread function is mathematically approximated with a 2D-gaussian distribution. This distribution is used to fit the spots imaged in the raw data to find their centres. These centres are used as an estimate of the location of the fluorophore underlying the diffraction-limited spot and are all overlaid in a single image, forming the reconstructed superresolution image. Similarly, raw SIM data is in essence composed of partial (because of the excitation with a 3D pattern of light rather than a continuous beam) widefield images overlaid with the even larger Moiré patterns that have a worse resolution than typical confocal images (Fig. 5b). Also here, elaborate data analysis is required, involving fourier transformations, the shifting of the information contained in the imaged Moiré patterns back into its original high frequency position and integration of multiple raw images, to reconstruct a single high resolution SIM image (Fig. 5c).

Because of the heavy reliance of PALM, STORM and SIM on data analysis tech-

1

niques, with the widespread implementation of these techniques, the widespread availability of advanced data analysis techniques also became necessary and the interest in advanced data analysis increased. With increased availability and interest, it is only natural that the image analysis of data acquired through other imaging techniques also improved, allowing more data to be extracted from these images too. A good example of this is the increased use of deconvolution software, where out of focus light is removed using image analysis software to create a three-dimensional image with improved contrast and resolution<sup>165</sup>. The increased availability and knowledge of data analysis techniques also allowed researchers to develop their own image processing or visualisation techniques. This process has been sped up by the availability of free open-source software such as ImageJ<sup>166</sup> and its framework Fiji<sup>167</sup>, which allows researchers to focus on information within the image most relevant to their particular research question, by building with relative ease their own image analysis software, or adapt and build upon the image analysis methods developed by others. Especially by improving quantification, which increased the potential for reliable comparison between different conditions, this development has contributed strongly to many important scientific advances in the field of biology<sup>168</sup>. Therefore the contribution of image analysis software, including its free open-source versions, has contributed as much to the current importance of light microscopy to biology as the technological advances in light microscopes and fluorophores.

## References

- 1 Yamada, K. M. & Geiger, B. Molecular interactions in cell adhesion complexes. *Current opinion in cell biology* 9, 76-85 (1997).
- 2 Geiger, B., Bershadsky, A., Pankov, R. & Yamada, K. M. Transmembrane crosstalk between the extracellular matrix--cytoskeleton crosstalk. *Nature reviews. Molecular cell biology* 2, 793-805, doi:10.1038/35099066 (2001).
- 3 Kanchanawong, P. *et al.* Nanoscale architecture of integrin-based cell adhesions. *Nature* 468, 580-584, doi:10.1038/nature09621 (2010).
- 4 Kim, D.-H. & Wirtz, D. Focal adhesion size uniquely predicts cell migration. *FASEB journal : official publication of the Federation of American Societies for Experimental Biology* 27, 1351-1361, doi:10.1096/fj.12-220160 (2013).
- 5 Burridge, K. & Guilluy, C. Focal adhesions, stress fibers and mechanical tension. *Experimental cell research* 343, 14-20, doi:10.1016/j.yexcr.2015.10.029 (2016).
- 6 Balaban, N. Q. *et al.* Force and focal adhesion assembly: a close relationship studied using elastic micropatterned substrates. *Nature cell biology* 3, 466-472, doi:10.1038/35074532 (2001).
- 7 Beningo, K. A., Dembo, M., Kaverina, I., Small, J. V. & Wang, Y. L. Nascent focal adhesions are responsible for the generation of strong propulsive forces in migrating fibroblasts. *The Journal of cell biology* 153, 881-888 (2001).
- 8 Tadokoro, S. *et al.* Talin binding to integrin beta tails: a final common step in integrin activation. *Science (New York, N.Y.)* 302, 103-106, doi:10.1126/science.1086652 (2003).
- 9 Chrzanowska-Wodnicka, M. & Burridge, K. Rho-stimulated contractility drives the forma-



- tion of stress fibers and focal adhesions. *The Journal of cell biology* 133, 1403-1415 (1996).
- 10 Rivelino, D. *et al.* Focal contacts as mechanosensors: externally applied local mechanical force induces growth of focal contacts by an mDia1-dependent and ROCK-independent mechanism. *The Journal of cell biology* 153, 1175-1186 (2001).
  - 11 Wang, H. B., Dembo, M., Hanks, S. K. & Wang, Y. Focal adhesion kinase is involved in mechanosensing during fibroblast migration. *Proceedings of the National Academy of Sciences of the United States of America* 98, 11295-11300, doi:10.1073/pnas.201201198 (2001).
  - 12 Galbraith, C. G., Yamada, K. M. & Sheetz, M. P. The relationship between force and focal complex development. *The Journal of cell biology* 159, 695-705, doi:10.1083/jcb.200204153 (2002).
  - 13 Kaverina, I. *et al.* Tensile stress stimulates microtubule outgrowth in living cells. *Journal of cell science* 115, 2283-2291 (2002).
  - 14 Pasapera, A. M., Schneider, I. C., Rericha, E., Schlaepfer, D. D. & Waterman, C. M. Myosin II activity regulates vinculin recruitment to focal adhesions through FAK-mediated paxillin phosphorylation. *The Journal of cell biology* 188, 877-890, doi:10.1083/jcb.200906012 (2010).
  - 15 Winograd-Katz, S. E., Fassler, R., Geiger, B. & Legate, K. R. The integrin adhesome: from genes and proteins to human disease. *Nature reviews. Molecular cell biology* 15, 273-288, doi:10.1038/nrm3769 (2014).
  - 16 Engler, A. J., Sen, S., Sweeney, H. L. & Discher, D. E. Matrix elasticity directs stem cell lineage specification. *Cell* 126, 677-689, doi:10.1016/j.cell.2006.06.044 (2006).
  - 17 Thiery, J. P. Cell adhesion in development: a complex signaling network. *Curr Opin Genet Dev* 13, 365-371, doi:10.1016/s0959-437x(03)00088-1 (2003).
  - 18 Maartens, A. P. & Brown, N. H. The many faces of cell adhesion during Drosophila muscle development. *Developmental biology* 401, 62-74, doi:10.1016/j.ydbio.2014.12.038 (2015).
  - 19 Wahl, S. M., Feldman, G. M. & McCarthy, J. B. Regulation of leukocyte adhesion and signaling in inflammation and disease. *Journal of leukocyte biology* 59, 789-796 (1996).
  - 20 Mitra, S. K. & Schlaepfer, D. D. Integrin-regulated FAK-Src signaling in normal and cancer cells. *Current opinion in cell biology* 18, 516-523, doi:10.1016/j.ceb.2006.08.011 (2006).
  - 21 Bianchi-Smiraglia, A., Paesante, S. & Bakin, A. V. Integrin beta5 contributes to the tumorigenic potential of breast cancer cells through the Src-FAK and MEK-ERK signaling pathways. *Oncogene* 32, 3049-3058, doi:10.1038/onc.2012.320 (2013).
  - 22 Lau, S. K. *et al.* EGFR-mediated carcinoma cell metastasis mediated by integrin alphavbeta5 depends on activation of c-Src and cleavage of MUC1. *PLoS one* 7, e36753, doi:10.1371/journal.pone.0036753 (2012).
  - 23 Bianconi, D., Unseld, M. & Prager, G. W. Integrins in the Spotlight of Cancer. *International journal of molecular sciences* 17, doi:10.3390/ijms17122037 (2016).
  - 24 Ata, R. & Antonescu, C. N. Integrins and Cell Metabolism: An Intimate Relationship Impacting Cancer. *International journal of molecular sciences* 18, doi:10.3390/ijms18010189 (2017).
  - 25 Desgrosellier, J. S. & Cheresch, D. A. Integrins in cancer: biological implications and therapeutic opportunities. *Nature reviews. Cancer* 10, 9-22, doi:10.1038/nrc2748 (2010).
  - 26 Xu, F., Zhang, J., Hu, G., Liu, L. & Liang, W. Hypoxia and TGF- $\beta$ 1 induced PLOD2 expression improve the migration and invasion of cervical cancer cells by promoting epithelial-to-mesenchymal transition (EMT) and focal adhesion formation. *Cancer Cell Int* 17, 54-54, doi:10.1186/s12935-017-0420-z (2017).
  - 27 Eckert, M. A. *et al.* ADAM12 induction by Twist1 promotes tumor invasion and metastasis via regulation of invadopodia and focal adhesions. *Journal of cell science* 130, 2036-2048, doi:10.1242/jcs.198200 (2017).
  - 28 Wipff, P.-J. & Hinz, B. Integrins and the activation of latent transforming growth factor beta1 - an intimate relationship. *Eur J Cell Biol* 87, 601-615, doi:10.1016/j.ejcb.2008.01.012 (2008).
  - 29 Bianchi-Smiraglia, A. *et al.* Integrin-beta5 and zyxin mediate formation of ventral stress

fibers in response to transforming growth factor beta. *Cell cycle (Georgetown, Tex.)* 12, 3377-3389, doi:10.4161/cc.26388 (2013).

30 Bianchi, A., Gervasi, M. E. & Bakin, A. Role of beta5-integrin in epithelial-mesenchymal transition in response to TGF-beta. *Cell cycle (Georgetown, Tex.)* 9, 1647-1659, doi:10.4161/cc.9.8.11517 (2010).

31 Lamouille, S., Xu, J. & Derynck, R. Molecular mechanisms of epithelial-mesenchymal transition. *Nature reviews. Molecular cell biology* 15, 178-196, doi:10.1038/nrm3758 (2014).

32 Berrier, A. L. & Yamada, K. M. Cell-matrix adhesion. *Journal of cellular physiology* 213, 565-573, doi:10.1002/jcp.21237 (2007).

33 Geiger, B. & Yamada, K. M. Molecular architecture and function of matrix adhesions. *Cold Spring Harb Perspect Biol* 3, a005033, doi:10.1101/cshperspect.a005033 (2011).

34 Lavelin, I. *et al.* Differential effect of actomyosin relaxation on the dynamic properties of focal adhesion proteins. *PLoS one* 8, e73549, doi:10.1371/journal.pone.0073549 (2013).

35 Theocharis, A. D., Skandalis, S. S., Gialeli, C. & Karamanos, N. K. Extracellular matrix structure. *Adv Drug Deliv Rev* 97, 4-27, doi:10.1016/j.addr.2015.11.001 (2016).

36 Adutler-Lieber, S. *et al.* Engineering of synthetic cellular microenvironments: implications for immunity. *Journal of autoimmunity* 54, 100-111, doi:10.1016/j.jaut.2014.05.003 (2014).

37 Chautard, E., Fatoux-Ardore, M., Ballut, L., Thierry-Mieg, N. & Ricard-Blum, S. MatrixDB, the extracellular matrix interaction database. *Nucleic acids research* 39, D235-240, doi:10.1093/nar/gkq830 (2011).

38 Doyle, A. D., Carvajal, N., Jin, A., Matsumoto, K. & Yamada, K. M. Local 3D matrix microenvironment regulates cell migration through spatiotemporal dynamics of contractility-dependent adhesions. *Nature communications* 6, 8720, doi:10.1038/ncomms9720 (2015).

39 Singer, I. I., Kawka, D. W., Kazakis, D. M. & Clark, R. A. In vivo co-distribution of fibronectin and actin fibers in granulation tissue: immunofluorescence and electron microscope studies of the fibronexus at the myofibroblast surface. *The Journal of cell biology* 98, 2091-2106, doi:10.1083/jcb.98.6.2091 (1984).

40 Gunawan, F. *et al.* Focal adhesions are essential to drive zebrafish heart valve morphogenesis. *The Journal of cell biology* 218, 1039-1054, doi:10.1083/jcb.201807175 (2019).

41 Fischer, R. S., Lam, P.-Y., Huttenlocher, A. & Waterman, C. M. Filopodia and focal adhesions: An integrated system driving branching morphogenesis in neuronal pathfinding and angiogenesis. *Developmental biology* 451, 86-95, doi:10.1016/j.ydbio.2018.08.015 (2019).

42 Yue, J. *et al.* In vivo epidermal migration requires focal adhesion targeting of ACF7. *Nature communications* 7, 11692-11692, doi:10.1038/ncomms11692 (2016).

43 Haage, A. *et al.* Talin Autoinhibition Regulates Cell-ECM Adhesion Dynamics and Wound Healing In Vivo. *Cell Rep* 25, 2401-2416.e2405, doi:10.1016/j.celrep.2018.10.098 (2018).

44 Curtis, A. S. THE MECHANISM OF ADHESION OF CELLS TO GLASS. A STUDY BY INTERFERENCE REFLECTION MICROSCOPY. *The Journal of cell biology* 20, 199-215, doi:10.1083/jcb.20.2.199 (1964).

45 Abercrombie, M., Heaysman, J. E. & Pegrum, S. M. The locomotion of fibroblasts in culture. I. Movements of the leading edge. *Experimental cell research* 59, 393-398, doi:10.1016/0014-4827(70)90646-4 (1970).

46 Abercrombie, M., Heaysman, J. E. & Pegrum, S. M. The locomotion of fibroblasts in culture. II. "RRuffling". *Experimental cell research* 60, 437-444, doi:10.1016/0014-4827(70)90537-9 (1970).

47 Burridge, K. & Feramisco, J. R. Microinjection and localization of a 130K protein in living fibroblasts: a relationship to actin and fibronectin. *Cell* 19, 587-595, doi:10.1016/s0092-8674(80)80035-3 (1980).

48 Geiger, B. A 130K protein from chicken gizzard: its localization at the termini of microfilament bundles in cultured chicken cells. *Cell* 18, 193-205, doi:10.1016/0092-8674(79)90368-4 (1979).

- 49 Zaidel-Bar, R., Itzkovitz, S., Ma'ayan, A., Iyengar, R. & Geiger, B. Functional atlas of the integrin adhesome. *Nature cell biology* 9, 858-867, doi:10.1038/ncb0807-858 (2007).
- 50 Kuo, J.-C., Han, X., Hsiao, C.-T., Yates, J. R., 3rd & Waterman, C. M. Analysis of the myosin-II-responsive focal adhesion proteome reveals a role for  $\beta$ -Pix in negative regulation of focal adhesion maturation. *Nature cell biology* 13, 383-393, doi:10.1038/ncb2216 (2011).
- 51 Schiller, H. B., Friedel, C. C., Boulegue, C. & Fässler, R. Quantitative proteomics of the integrin adhesome show a myosin II-dependent recruitment of LIM domain proteins. *EMBO Rep* 12, 259-266, doi:10.1038/embor.2011.5 (2011).
- 52 Liu, J. *et al.* Talin determines the nanoscale architecture of focal adhesions. *Proceedings of the National Academy of Sciences of the United States of America* 112, E4864-4873, doi:10.1073/pnas.1512025112 (2015).
- 53 Paszek, M. J. *et al.* Scanning angle interference microscopy reveals cell dynamics at the nanoscale. *Nature methods* 9, 825-827, doi:10.1038/nmeth.2077 (2012).
- 54 Stubb, A. *et al.* Superresolution architecture of cornerstone focal adhesions in human pluripotent stem cells. *Nature communications* 10, 4756, doi:10.1038/s41467-019-12611-w (2019).
- 55 Orré, T., Rossier, O. & Giannone, G. The inner life of integrin adhesion sites: From single molecules to functional macromolecular complexes. *Experimental cell research* 379, 235-244, doi:10.1016/j.yexcr.2019.03.036 (2019).
- 56 Small, J. V., Rottner, K., Kaverina, I. & Anderson, K. I. Assembling an actin cytoskeleton for cell attachment and movement. *Biochimica et biophysica acta* 1404, 271-281 (1998).
- 57 Wu, C., Keivens, V. M., O'Toole, T. E., McDonald, J. A. & Ginsberg, M. H. Integrin activation and cytoskeletal interaction are essential for the assembly of a fibronectin matrix. *Cell* 83, 715-724, doi:10.1016/0092-8674(95)90184-1 (1995).
- 58 Kechagia, J. Z., Ivaska, J. & Roca-Cusachs, P. Integrins as biomechanical sensors of the microenvironment. *Nature reviews. Molecular cell biology* 20, 457-473, doi:10.1038/s41580-019-0134-2 (2019).
- 59 Shattil, S. J., Kim, C. & Ginsberg, M. H. The final steps of integrin activation: the end game. *Nature reviews. Molecular cell biology* 11, 288-300, doi:10.1038/nrm2871 (2010).
- 60 Laukaitis, C. M., Webb, D. J., Donais, K. & Horwitz, A. F. Differential dynamics of alpha 5 integrin, paxillin, and alpha-actinin during formation and disassembly of adhesions in migrating cells. *The Journal of cell biology* 153, 1427-1440 (2001).
- 61 Webb, D. J. *et al.* FAK-Src signalling through paxillin, ERK and MLCK regulates adhesion disassembly. *Nature cell biology* 6, 154-161, doi:10.1038/ncb1094 (2004).
- 62 Wiseman, P. W. *et al.* Spatial mapping of integrin interactions and dynamics during cell migration by image correlation microscopy. *Journal of cell science* 117, 5521-5534, doi:10.1242/jcs.01416 (2004).
- 63 Bellis, S. L., Miller, J. T. & Turner, C. E. Characterization of tyrosine phosphorylation of paxillin in vitro by focal adhesion kinase. *The Journal of biological chemistry* 270, 17437-17441 (1995).
- 64 Brown, M. C., Perrotta, J. A. & Turner, C. E. Identification of LIM3 as the principal determinant of paxillin focal adhesion localization and characterization of a novel motif on paxillin directing vinculin and focal adhesion kinase binding. *The Journal of cell biology* 135, 1109-1123 (1996).
- 65 Schaller, M. D. & Parsons, J. T. pp125FAK-dependent tyrosine phosphorylation of paxillin creates a high-affinity binding site for Crk. *Molecular and cellular biology* 15, 2635-2645 (1995).
- 66 Richardson, A., Malik, R. K., Hildebrand, J. D. & Parsons, J. T. Inhibition of cell spreading by expression of the C-terminal domain of focal adhesion kinase (FAK) is rescued by coexpression of Src or catalytically inactive FAK: a role for paxillin tyrosine phosphorylation. *Molecular and cellular biology* 17, 6906-6914 (1997).
- 67 Tsubouchi, A. *et al.* Localized suppression of RhoA activity by Tyr31/118-phosphorylated paxillin in cell adhesion and migration. *The Journal of cell biology* 159, 673-683, doi:10.1083/jcb.200202117 (2002).

- 68 Brown, M. C. & Turner, C. E. Paxillin: adapting to change. *Physiological reviews* 84, 1315-1339, doi:10.1152/physrev.00002.2004 (2004).
- 69 Wang, Y. & Gilmore, T. D. Zyxin and paxillin proteins: focal adhesion plaque LIM domain proteins go nuclear. *Biochimica et biophysica acta* 1593, 115-120 (2003).
- 70 Sen, A. *et al.* Paxillin mediates extranuclear and intranuclear signaling in prostate cancer proliferation. *The Journal of Clinical Investigation* 122, 2469-2481, doi:10.1172/JCI62044 (2012).
- 71 Woods, A. J. *et al.* Paxillin associates with poly(A)-binding protein 1 at the dense endoplasmic reticulum and the leading edge of migrating cells. *The Journal of biological chemistry* 277, 6428-6437, doi:10.1074/jbc.M109446200 (2002).
- 72 Woods, A. J., Kantidakis, T., Sabe, H., Critchley, D. R. & Norman, J. C. Interaction of paxillin with poly(A)-binding protein 1 and its role in focal adhesion turnover and cell migration. *Molecular and cellular biology* 25, 3763-3773, doi:10.1128/mcb.25.9.3763-3773.2005 (2005).
- 73 Hagel, M. *et al.* The adaptor protein paxillin is essential for normal development in the mouse and is a critical transducer of fibronectin signaling. *Molecular and cellular biology* 22, 901-915 (2002).
- 74 Choi, C. K. *et al.* Actin and alpha-actinin orchestrate the assembly and maturation of nascent adhesions in a myosin II motor-independent manner. *Nature cell biology* 10, 1039-1050, doi:10.1038/ncb1763 (2008).
- 75 Drees, B. *et al.* Characterization of the interaction between zyxin and members of the Ena/vasodilator-stimulated phosphoprotein family of proteins. *The Journal of biological chemistry* 275, 22503-22511, doi:10.1074/jbc.M001698200 (2000).
- 76 Reinhard, M., Jouvenal, K., Tripier, D. & Walter, U. Identification, purification, and characterization of a zyxin-related protein that binds the focal adhesion and microfilament protein VASP (vasodilator-stimulated phosphoprotein). *Proceedings of the National Academy of Sciences of the United States of America* 92, 7956-7960 (1995).
- 77 Rottner, K., Krause, M., Gimona, M., Small, J. V. & Wehland, J. Zyxin is not colocalized with vasodilator-stimulated phosphoprotein (VASP) at lamellipodial tips and exhibits different dynamics to vinculin, paxillin, and VASP in focal adhesions. *Molecular biology of the cell* 12, 3103-3113 (2001).
- 78 Furman, C. *et al.* Ena/VASP is required for endothelial barrier function in vivo. *The Journal of cell biology* 179, 761-775, doi:10.1083/jcb.200705002 (2007).
- 79 Hirata, H., Tatsumi, H. & Sokabe, M. Zyxin emerges as a key player in the mechanotransduction at cell adhesive structures. *Communicative & integrative biology* 1, 192-195 (2008).
- 80 Smith, M. A. *et al.* A zyxin-mediated mechanism for actin stress fiber maintenance and repair. *Developmental cell* 19, 365-376, doi:10.1016/j.devcel.2010.08.008 (2010).
- 81 Nix, D. A. & Beckerle, M. C. Nuclear-cytoplasmic shuttling of the focal contact protein, zyxin: a potential mechanism for communication between sites of cell adhesion and the nucleus. *The Journal of cell biology* 138, 1139-1147 (1997).
- 82 Cattaruzza, M., Lattrich, C. & Hecker, M. Focal adhesion protein zyxin is a mechanosensitive modulator of gene expression in vascular smooth muscle cells. *Hypertension (Dallas, Tex. : 1979)* 43, 726-730, doi:10.1161/01.hyp.0000119189.82659.52 (2004).
- 83 Lele, T. P. *et al.* Mechanical forces alter zyxin unbinding kinetics within focal adhesions of living cells. *Journal of cellular physiology* 207, 187-194, doi:10.1002/jcp.20550 (2006).
- 84 Castello, A. *et al.* Insights into RNA biology from an atlas of mammalian mRNA-binding proteins. *Cell* 149, 1393-1406, doi:10.1016/j.cell.2012.04.031 (2012).
- 85 Hirata, H., Tatsumi, H. & Sokabe, M. Mechanical forces facilitate actin polymerization at focal adhesions in a zyxin-dependent manner. *Journal of cell science* 121, 2795-2804, doi:10.1242/jcs.030320 (2008).
- 86 Uemura, A., Nguyen, T. N., Steele, A. N. & Yamada, S. The LIM domain of zyxin is sufficient for force-induced accumulation of zyxin during cell migration. *Biophysical journal* 101, 1069-1075, doi:10.1016/j.bpj.2011.08.001 (2011).

- 87 Drees, B. E., Andrews, K. M. & Beckerle, M. C. Molecular dissection of zyxin function reveals its involvement in cell motility. *The Journal of cell biology* 147, 1549-1560 (1999).
- 88 Crawford, A. W., Michelsen, J. W. & Beckerle, M. C. An interaction between zyxin and alpha-actinin. *The Journal of cell biology* 116, 1381-1393 (1992).
- 89 Yoshigi, M., Hoffman, L. M., Jensen, C. C., Yost, H. J. & Beckerle, M. C. Mechanical force mobilizes zyxin from focal adhesions to actin filaments and regulates cytoskeletal reinforcement. *The Journal of cell biology* 171, 209-215, doi:10.1083/jcb.200505018 (2005).
- 90 Hoffman, L. M. *et al.* Genetic ablation of zyxin causes Mena/VASP mislocalization, increased motility, and deficits in actin remodeling. *The Journal of cell biology* 172, 771-782, doi:10.1083/jcb.200512115 (2006).
- 91 Golsteyn, R. M., Beckerle, M. C., Koay, T. & Friederich, E. Structural and functional similarities between the human cytoskeletal protein zyxin and the ActA protein of *Listeria monocytogenes*. *Journal of cell science* 110 ( Pt 16), 1893-1906 (1997).
- 92 Nix, D. A. *et al.* Targeting of zyxin to sites of actin membrane interaction and to the nucleus. *The Journal of biological chemistry* 276, 34759-34767, doi:10.1074/jbc.M102820200 (2001).
- 93 Fradelizi, J. *et al.* ActA and human zyxin harbour Arp2/3-independent actin-polymerization activity. *Nature cell biology* 3, 699-707, doi:10.1038/35087009 (2001).
- 94 Bear, J. E. & Gertler, F. B. Ena/VASP: towards resolving a pointed controversy at the barbed end. *Journal of cell science* 122, 1947-1953, doi:10.1242/jcs.038125 (2009).
- 95 Brühmann, S. *et al.* Distinct VASP tetramers synergize in the processive elongation of individual actin filaments from clustered arrays. *Proceedings of the National Academy of Sciences of the United States of America* 114, E5815-e5824, doi:10.1073/pnas.1703145114 (2017).
- 96 Damiano-Guercio, J. *et al.* Loss of Ena/VASP interferes with lamellipodium architecture, motility and integrin-dependent adhesion. *eLife* 9, doi:10.7554/eLife.55351 (2020).
- 97 Hoffman, L. M. *et al.* Targeted disruption of the murine zyxin gene. *Molecular and cellular biology* 23, 70-79 (2003).
- 98 Bubb, M. R., Spector, I., Beyer, B. B. & Fosen, K. M. Effects of jasplakinolide on the kinetics of actin polymerization. An explanation for certain in vivo observations. *The Journal of biological chemistry* 275, 5163-5170 (2000).
- 99 Amsellem, V. *et al.* The actin cytoskeleton-associated protein zyxin acts as a tumor suppressor in Ewing tumor cells. *Experimental cell research* 304, 443-456, doi:10.1016/j.yexcr.2004.10.035 (2005).
- 100 Sanchez-Carbayo, M. *et al.* Molecular profiling of bladder cancer using cDNA microarrays: defining histogenesis and biological phenotypes. *Cancer research* 62, 6973-6980 (2002).
- 101 Wang, W. *et al.* Analysis of methylation-sensitive transcriptome identifies GADD45a as a frequently methylated gene in breast cancer. *Oncogene* 24, 2705-2714, doi:10.1038/sj.onc.1208464 (2005).
- 102 Humphries, J. D. *et al.* Vinculin controls focal adhesion formation by direct interactions with talin and actin. *The Journal of cell biology* 179, 1043-1057, doi:10.1083/jcb.200703036 (2007).
- 103 Bakolitsa, C. *et al.* Structural basis for vinculin activation at sites of cell adhesion. *Nature* 430, 583-586, doi:10.1038/nature02610 (2004).
- 104 Jones, P. *et al.* Identification of a talin binding site in the cytoskeletal protein vinculin. *The Journal of cell biology* 109, 2917-2927 (1989).
- 105 Opazo Saez, A. *et al.* Tension development during contractile stimulation of smooth muscle requires recruitment of paxillin and vinculin to the membrane. *American journal of physiology. Cell physiology* 286, C433-447, doi:10.1152/ajpcell.00030.2003 (2004).
- 106 Thomas, S. M., Hagel, M. & Turner, C. E. Characterization of a focal adhesion protein, Hic-5, that shares extensive homology with paxillin. *Journal of cell science* 112 ( Pt 2), 181-190 (1999).
- 107 Sathe, A. R., Shivashankar, G. V. & Sheetz, M. P. Nuclear transport of paxillin depends on focal adhesion dynamics and FAT domains. *Journal of cell science* 129, 1981-1988, doi:10.1242/jcs.172643

(2016).

108 Gertler, F. B., Niebuhr, K., Reinhard, M., Wehland, J. & Soriano, P. Mena, a relative of VASP and Drosophila Enabled, is implicated in the control of microfilament dynamics. *Cell* 87, 227-239 (1996).

109 Brindle, N. P., Holt, M. R., Davies, J. E., Price, C. J. & Critchley, D. R. The focal-adhesion vasodilator-stimulated phosphoprotein (VASP) binds to the proline-rich domain in vinculin. *The Biochemical journal* 318 ( Pt 3), 753-757 (1996).

110 Reinhard, M., Rudiger, M., Jockusch, B. M. & Walter, U. VASP interaction with vinculin: a recurring theme of interactions with proline-rich motifs. *FEBS letters* 399, 103-107 (1996).

111 McGregor, A., Blanchard, A. D., Rowe, A. J. & Critchley, D. R. Identification of the vinculin-binding site in the cytoskeletal protein alpha-actinin. *The Biochemical journal* 301 ( Pt 1), 225-233 (1994).

112 Xu, W., Baribault, H. & Adamson, E. D. Vinculin knockout results in heart and brain defects during embryonic development. *Development (Cambridge, England)* 125, 327-337 (1998).

113 Volberg, T. *et al.* Focal adhesion formation by F9 embryonal carcinoma cells after vinculin gene disruption. *Journal of cell science* 108 ( Pt 6), 2253-2260 (1995).

114 Xu, W., Coll, J. L. & Adamson, E. D. Rescue of the mutant phenotype by reexpression of full-length vinculin in null F9 cells; effects on cell locomotion by domain deleted vinculin. *Journal of cell science* 111 ( Pt 11), 1535-1544 (1998).

115 Mierke, C. T. *et al.* Vinculin facilitates cell invasion into three-dimensional collagen matrices. *The Journal of biological chemistry* 285, 13121-13130, doi:10.1074/jbc.M109.087171 (2010).

116 Thievensen, I. *et al.* Vinculin-actin interaction couples actin retrograde flow to focal adhesions, but is dispensable for focal adhesion growth. *The Journal of cell biology* 202, 163-177, doi:10.1083/jcb.201303129 (2013).

117 Coltella, N. *et al.* Role of the MET/HGF receptor in proliferation and invasive behavior of osteosarcoma. *FASEB journal : official publication of the Federation of American Societies for Experimental Biology* 17, 1162-1164, doi:10.1096/fj.02-0576fje (2003).

118 Patane, S. *et al.* MET overexpression turns human primary osteoblasts into osteosarcomas. *Cancer research* 66, 4750-4757, doi:10.1158/0008-5472.Can-05-4422 (2006).

119 Patane, S. *et al.* A new Met inhibitory-scaffold identified by a focused forward chemical biological screen. *Biochemical and biophysical research communications* 375, 184-189, doi:10.1016/j.bbrc.2008.07.159 (2008).

120 Pennacchietti, S. *et al.* Hypoxia promotes invasive growth by transcriptional activation of the met protooncogene. *Cancer cell* 3, 347-361 (2003).

121 Bottaro, D. P. *et al.* Identification of the hepatocyte growth factor receptor as the c-met proto-oncogene product. *Science (New York, N.Y.)* 251, 802-804, doi:10.1126/science.1846706 (1991).

122 Stoker, M., Gherardi, E., Perryman, M. & Gray, J. Scatter factor is a fibroblast-derived modulator of epithelial cell mobility. *Nature* 327, 239-242, doi:10.1038/327239a0 (1987).

123 Weidner, K. M., Behrens, J., Vandekerckhove, J. & Birchmeier, W. Scatter factor: molecular characteristics and effect on the invasiveness of epithelial cells. *The Journal of cell biology* 111, 2097-2108, doi:10.1083/jcb.111.5.2097 (1990).

124 Park, M. *et al.* Sequence of MET protooncogene cDNA has features characteristic of the tyrosine kinase family of growth-factor receptors. *Proceedings of the National Academy of Sciences* 84, 6379-6383, doi:10.1073/pnas.84.18.6379 (1987).

125 Birchmeier, C., Birchmeier, W., Gherardi, E. & Vande Woude, G. F. Met, metastasis, motility and more. *Nature Reviews Molecular Cell Biology* 4, 915-925, doi:10.1038/nrm1261 (2003).

126 Imamura, R. & Matsumoto, K. Hepatocyte growth factor in physiology and infectious diseases. *Cytokine* 98, 97-106, doi:10.1016/j.cyt.2016.12.025 (2017).

127 Cecchi, F., Rabe, D. C. & Bottaro, D. P. Targeting the HGF/Met signalling pathway in can-

- cer. *Eur J Cancer* 46, 1260-1270, doi:10.1016/j.ejca.2010.02.028 (2010).
- 128 Scagliotti, G. V., Novello, S. & von Pawel, J. The emerging role of MET/HGF inhibitors in oncology. *Cancer Treat Rev* 39, 793-801, doi:10.1016/j.ctrv.2013.02.001 (2013).
- 129 Trusolino, L. & Comoglio, P. M. Scatter-factor and semaphorin receptors: cell signalling for invasive growth. *Nature reviews. Cancer* 2, 289-300, doi:10.1038/nrc779 (2002).
- 130 Whang, Y. M., Jung, S. P., Kim, M. K., Chang, I. H. & Park, S. I. Targeting the Hepatocyte Growth Factor and c-Met Signaling Axis in Bone Metastases. *International journal of molecular sciences* 20, doi:10.3390/ijms20020384 (2019).
- 131 Cheng, F. & Guo, D. MET in glioma: signaling pathways and targeted therapies. *J Exp Clin Cancer Res* 38, 270, doi:10.1186/s13046-019-1269-x (2019).
- 132 Zhang, H., Feng, Q., Chen, W. D. & Wang, Y. D. HGF/c-MET: A Promising Therapeutic Target in the Digestive System Cancers. *International journal of molecular sciences* 19, doi:10.3390/ijms19113295 (2018).
- 133 Boros, P. & Miller, C. M. Hepatocyte growth factor: a multifunctional cytokine. *Lancet* 345, 293-295, doi:10.1016/s0140-6736(95)90279-1 (1995).
- 134 Zarnegar, R. & Michalopoulos, G. K. The many faces of hepatocyte growth factor: from hepatopoiesis to hematopoiesis. *The Journal of cell biology* 129, 1177-1180, doi:10.1083/jcb.129.5.1177 (1995).
- 135 Cox, I. J. & Sheppard, C. J. Scanning optical microscope incorporating a digital framestore and microcomputer. *Appl Opt* 22, 1474-1474, doi:10.1364/ao.22.001474 (1983).
- 136 Brakenhoff, G. J., van der Voort, H. T., van Spronsen, E. A., Linnemans, W. A. & Nanninga, N. Three-dimensional chromatin distribution in neuroblastoma nuclei shown by confocal scanning laser microscopy. *Nature* 317, 748-749, doi:10.1038/317748a0 (1985).
- 137 Shimomura, O., Johnson, F. H. & Saiga, Y. Extraction, purification and properties of aequorin, a bioluminescent protein from the luminous hydromedusa, *Aequorea*. *J Cell Comp Physiol* 59, 223-239, doi:10.1002/jcp.1030590302 (1962).
- 138 Tsien, R. Y. The green fluorescent protein. *Annu Rev Biochem* 67, 509-544, doi:10.1146/annurev.biochem.67.1.509 (1998).
- 139 Axelrod, D. Cell-substrate contacts illuminated by total internal reflection fluorescence. *The Journal of cell biology* 89, 141-145, doi:10.1083/jcb.89.1.141 (1981).
- 140 Stout, A. L. & Axelrod, D. Evanescent field excitation of fluorescence by epi-illumination microscopy. *Appl Opt* 28, 5237-5242, doi:10.1364/ao.28.005237 (1989).
- 141 Gustafsson, M. G. Surpassing the lateral resolution limit by a factor of two using structured illumination microscopy. *J Microsc* 198, 82-87 (2000).
- 142 Schermelleh, L., Heintzmann, R. & Leonhardt, H. A guide to super-resolution fluorescence microscopy. *The Journal of cell biology* 190, 165-175, doi:10.1083/jcb.201002018 (2010).
- 143 Walde, M., Monypenny, J., Heintzmann, R., Jones, G. E. & Cox, S. Vinculin binding angle in podosomes revealed by high resolution microscopy. *PLoS one* 9, e88251, doi:10.1371/journal.pone.0088251 (2014).
- 144 de Boer, P., Hoogenboom, J. P. & Giepmans, B. N. Correlated light and electron microscopy: ultrastructure lights up! *Nature methods* 12, 503-513, doi:10.1038/nmeth.3400 (2015).
- 145 Zonneville, A. C. *et al.* Integration of a high-NA light microscope in a scanning electron microscope. *J Microsc* 252, 58-70, doi:10.1111/jmi.12071 (2013).
- 146 Wouters, C. H. & Koerten, H. K. Combined light microscope and scanning electron microscope, a new instrument for cell biology. *Cell Biol Int Rep* 6, 955-959, doi:10.1016/0309-1651(82)90007-8 (1982).
- 147 Axelrod, D., Koppel, D. E., Schlessinger, J., Elson, E. & Webb, W. W. Mobility measurement by analysis of fluorescence photobleaching recovery kinetics. *Biophysical journal* 16, 1055-1069, doi:10.1016/s0006-3495(76)85755-4 (1976).

- 148 Koppel, D. E., Axelrod, D., Schlessinger, J., Elson, E. L. & Webb, W. W. Dynamics of fluorescence marker concentration as a probe of mobility. *Biophysical journal* 16, 1315-1329, doi:10.1016/s0006-3495(76)85776-1 (1976).
- 149 Peters, R., Peters, J., Tews, K. H. & Bähr, W. A microfluorimetric study of translational diffusion in erythrocyte membranes. *Biochimica et biophysica acta* 367, 282-294, doi:10.1016/0005-2736(74)90085-6 (1974).
- 150 Houtsmuller, A. B. *et al.* Action of DNA repair endonuclease ERCC1/XPF in living cells. *Science (New York, N.Y.)* 284, 958-961, doi:10.1126/science.284.5416.958 (1999).
- 151 Phair, R. D. & Misteli, T. High mobility of proteins in the mammalian cell nucleus. *Nature* 404, 604-609, doi:10.1038/35007077 (2000).
- 152 McNally, J. G., Müller, W. G., Walker, D., Wolford, R. & Hager, G. L. The glucocorticoid receptor: rapid exchange with regulatory sites in living cells. *Science (New York, N.Y.)* 287, 1262-1265, doi:10.1126/science.287.5456.1262 (2000).
- 153 Stenoién, D. L. *et al.* FRAP reveals that mobility of oestrogen receptor- $\alpha$  is ligand- and proteasome-dependent. *Nature cell biology* 3, 15-23, doi:10.1038/35050515 (2001).
- 154 Mochizuki, N. *et al.* Spatio-temporal images of growth-factor-induced activation of Ras and Rap1. *Nature* 411, 1065-1068, doi:10.1038/35082594 (2001).
- 155 Geverts, B., van Royen, M. E. & Houtsmuller, A. B. Analysis of biomolecular dynamics by FRAP and computer simulation. *Methods in molecular biology (Clifton, N.J.)* 1251, 109-133, doi:10.1007/978-1-4939-2080-8\_7 (2015).
- 156 Carrero, G., McDonald, D., Crawford, E., de Vries, G. & Hendzel, M. J. Using FRAP and mathematical modeling to determine the in vivo kinetics of nuclear proteins. *Methods* 29, 14-28, doi:10.1016/s1046-2023(02)00288-8 (2003).
- 157 Shcherbakova, D. M. & Verkhusha, V. V. Chromophore chemistry of fluorescent proteins controlled by light. *Curr Opin Chem Biol* 20, 60-68, doi:10.1016/j.cbpa.2014.04.010 (2014).
- 158 Lukyanov, K. A., Chudakov, D. M., Lukyanov, S. & Verkhusha, V. V. Innovation: Photoactivatable fluorescent proteins. *Nature reviews. Molecular cell biology* 6, 885-891, doi:10.1038/nrm1741 (2005).
- 159 Patterson, G. H. & Lippincott-Schwartz, J. A photoactivatable GFP for selective photolabeling of proteins and cells. *Science (New York, N.Y.)* 297, 1873-1877, doi:10.1126/science.1074952 (2002).
- 160 Nienhaus, K. & Nienhaus, G. U. Fluorescent proteins for live-cell imaging with super-resolution. *Chem Soc Rev* 43, 1088-1106, doi:10.1039/c3cs60171d (2014).
- 161 Wang, S., Moffitt, J. R., Dempsey, G. T., Xie, X. S. & Zhuang, X. Characterization and development of photoactivatable fluorescent proteins for single-molecule-based superresolution imaging. *Proceedings of the National Academy of Sciences of the United States of America* 111, 8452-8457, doi:10.1073/pnas.1406593111 (2014).
- 162 Betzig, E. *et al.* Imaging intracellular fluorescent proteins at nanometer resolution. *Science (New York, N.Y.)* 313, 1642-1645, doi:10.1126/science.1127344 (2006).
- 163 Rust, M. J., Bates, M. & Zhuang, X. Sub-diffraction-limit imaging by stochastic optical reconstruction microscopy (STORM). *Nature methods* 3, 793-795, doi:10.1038/nmeth929 (2006).
- 164 Hess, S. T., Girirajan, T. P. & Mason, M. D. Ultra-high resolution imaging by fluorescence photoactivation localization microscopy. *Biophysical journal* 91, 4258-4272, doi:10.1529/biophysj.106.091116 (2006).
- 165 Verdaasdonk, J. S., Stephens, A. D., Haase, J. & Bloom, K. Bending the rules: widefield microscopy and the Abbe limit of resolution. *Journal of cellular physiology* 229, 132-138, doi:10.1002/jcp.24439 (2014).
- 166 Schneider, C. A., Rasband, W. S. & Eliceiri, K. W. NIH Image to ImageJ: 25 years of image analysis. *Nature methods* 9, 671-675 (2012).
- 167 Schindelin, J. *et al.* Fiji: an open-source platform for biological-image analysis. *Nature meth-*



ods 9, 676-682, doi:10.1038/nmeth.2019 (2012).

168 Arena, E. T. *et al.* Quantitating the cell: turning images into numbers with ImageJ. *Wiley Interdiscip Rev Dev Biol* 6, doi:10.1002/wdev.260 (2017).

169 Berman, H. M. *et al.* The Protein Data Bank. *Nucleic acids research* 28, 235-242, doi:10.1093/nar/28.1.235 (2000).

170 Liang, M. *et al.* Structural basis of the target-binding mode of the G protein-coupled receptor kinase-interacting protein in the regulation of focal adhesion dynamics. *The Journal of biological chemistry* 294, 5827-5839, doi:10.1074/jbc.RA118.006915 (2019).

171 Zhu, L. *et al.* Structural Basis of Paxillin Recruitment by Kindlin-2 in Regulating Cell Adhesion. *Structure* 27, 1686-1697.e1685, doi:10.1016/j.str.2019.09.006 (2019).

172 Waterhouse, A. *et al.* SWISS-MODEL: homology modelling of protein structures and complexes. *Nucleic acids research* 46, W296-w303, doi:10.1093/nar/gky427 (2018).

173 Stokes, P. H. *et al.* Mutation in a flexible linker modulates binding affinity for modular complexes. *Proteins* 87, 425-429, doi:10.1002/prot.25675 (2019).

174 Ball, L. J. *et al.* Dual epitope recognition by the VASP EVH1 domain modulates polyproline ligand specificity and binding affinity. *The EMBO journal* 19, 4903-4914, doi:10.1093/emboj/19.18.4903 (2000).

175 Kühnel, K. *et al.* The VASP tetramerization domain is a right-handed coiled coil based on a 15-residue repeat. *Proceedings of the National Academy of Sciences of the United States of America* 101, 17027-17032, doi:10.1073/pnas.0403069101 (2004).

176 Izard, T. *et al.* Vinculin activation by talin through helical bundle conversion. *Nature* 427, 171-175, doi:10.1038/nature02281 (2004).



# Chapter 2

## Dynamics of paxillin, vinculin, zyxin and VASP depend on focal adhesion location and orientation

Karin Legerstee<sup>1</sup>, Bart Geverts<sup>1</sup>, and Adriaan B. Houtsmuller<sup>1</sup>

<sup>1</sup> Erasmus Medical Centre Rotterdam, Department of Pathology, Optical Imaging Centre, Rotterdam, The Netherlands.

Published as a part of:

Legerstee, K., Geverts, B., Slotman, J.A. et al. Dynamics and distribution of paxillin, vinculin, zyxin and VASP depend on focal adhesion location and orientation. *Sci Rep* 9, 10460 (2019)

## Abstract

Focal adhesions (FAs) are multiprotein structures that link the intracellular cytoskeleton to the extracellular matrix. They mediate cell adhesion and migration, crucial to many (patho-) physiological processes. We examined in two cell types from different species the binding dynamics of functionally related FA protein pairs: paxillin and vinculin versus zyxin and VASP. In both cell types, photo-bleaching experiments showed that ~40% of paxillin and vinculin remained stably associated with an FA for over half an hour, comparable to the average FA lifetime. Zyxin and VASP predominantly displayed more transient interactions. Furthermore, we show protein binding dynamics are influenced by FA location and orientation. In FAs located close to the edge of the adherent membrane paxillin, zyxin and VASP were more dynamic and had larger bound fractions. Zyxin and VASP were also more dynamic and had larger bound fractions at FAs perpendicular compared to parallel to this edge. The increased dynamic binding of the key structural factor paxillin may increase the dynamics of the FA complex as a whole, while the directly actin-binding zyxin and VASP potentially enhance the coupling of actin to these FAs.

## Introduction

Focal adhesions (FAs) are the main cellular structures linking the intracellular cytoskeleton to the extracellular matrix (ECM). They are typically several square micrometres in size<sup>1,2</sup>. On the membrane-facing side integrins, transmembrane receptors directly binding to the extracellular matrix (ECM), are the main FA components. A specialised form of actin linked to contractile myosin-II forms the edge of the FA on the cytoplasm-facing side, which we will refer to as F-actin. In between integrins and actin a large and diverse intracellular macromolecular protein assembly is present, with over 200 different reported proteins<sup>3,4</sup>. These include (trans)membrane receptors, other than integrins, adaptor proteins and many different signalling proteins such as kinases, phosphatases and G-protein regulators, which through post-translational modifications add significantly to FA complexity. FAs experience force, the strength of which depends on the combination of myosin-II contractility and the stiffness of the ECM. Because of their importance to the transmission of force from the cell to the ECM and in cell adhesion, FAs are crucial to cell migration. Migration and adhesion are key cellular functions required for many physiological and pathophysiological processes, like embryological development, the functioning of the immune system and also cancer, in particular metastasis<sup>4-6</sup>.

Here we investigated FA location and FA orientation dependent dynamics of four FA proteins, the large scaffold proteins paxillin and vinculin, and two FA proteins that are closely linked to the actin associated with FAs, zyxin and vasodilator-stimulated phosphoprotein (VASP). As adaptor proteins paxillin and vinculin are among the proteins with the most potential binding partners within FAs<sup>3</sup>. In keeping with their having a linking, structural, role they are amongst the first proteins to be recruited to assembling focal adhesion complexes, especially the directly integrin-binding paxillin<sup>7-11</sup>. Vinculin has a head and a tail domain with a flexible linker in between, allowing vinculin to adopt open and closed conformations<sup>12</sup>. Its head domain shares many important binding partners and functions with paxillin, indeed paxillin itself is one of its binding partners<sup>13-16</sup>. However, while Paxillin has no direct interaction with actin, vinculin's tail domain can directly bind actin filaments as well as the actin-binding proteins  $\alpha$ -actinin and the ENA/VASP-proteins<sup>16-20</sup>. Zyxin and VASP are recruited to assembling FAs at much later stages than paxillin or vinculin and are more closely linked to actin<sup>10</sup>. Apart from at FAs zyxin and VASP also cluster at actin-polymerisation complexes, which are periodically distributed along F-actin fibres<sup>21-23</sup>. To stimulate actin polymerisation along FAs zyxin, VASP and vinculin depend on each other for proper functioning<sup>24-29</sup>. Zyxin and VASP, without vinculin, also work

together in several other cellular processes such as efficient cell spreading and VASP depends on zyxin for its force-dependent recruitment to FAs<sup>25,30-32</sup>.

In photobleaching experiments ~40% of paxillin and vinculin remained stably associated with an FA for over half an hour. Zyxin and VASP predominantly displayed more transient interactions. We also reveal that the binding dynamics of VASP, zyxin, vinculin and paxillin differ with FA location and FA orientation relative to the closest edge of the ventral, or adherent, portion of the plasma membrane. Several factors form gradients based on their distance from the ventral membrane edge, such as actin fibre thickness and connectivity, the concentration of (signalling) molecules and enzyme activity<sup>33-40</sup>, effectively creating different local environments for FAs varying with their distance from the ventral membrane edge. Lastly, by using Monte Carlo based simulations we were able to provide a detailed quantification of the binding dynamics of these four proteins, as well as of the differences seen in FAs with different orientations or cellular locations<sup>41</sup>.

## Results

### Focal adhesion proteins have stably associated fractions at similar ratios across cell types

First, through FRAP-experiments we examined the binding dynamics of fluorescently-labelled paxillin, vinculin, VASP and zyxin at FAs in two different cell-types from two different species; U2OS cells, a human bone cancer cell line, and MDCK dog kidney cells (Fig. 1). Paxillin and vinculin both take about six minutes to reach final recovery levels at ~60% of prebleach fluorescence intensity, whereas both zyxin and VASP recover within two to three minutes to approximately 80 and 90% of prebleach fluorescence intensity. The same pattern of final recovery levels, highest for VASP, intermediate for zyxin and lowest and strikingly similar for vinculin and paxillin, was seen in both U2OS and MDCK cells. To facilitate comparison of recovery rates, irrespective of bleach depth or final recovery levels, recovery curves were expressed relative to intensity immediately after bleaching (0) and final recovery levels (1) (Fig. 1c,d). This highlights the much faster recovery rates of VASP and zyxin versus the highly similar slow recovery rates of paxillin and vinculin. Prolonged FRAP experiments verified paxillin recovery levels remained stable up to 15 minutes post-bleach (Supplementary Fig. S1). To rule out that the incomplete recoveries were due to bleaching of a significant portion of the cytoplasmic protein pool by the intense bleach pulse, we performed experiments where FAs were bleached a second time (Supplementary Fig. S2). If the bleach pulses bleached a significant portion of the protein pool, fluorescence recovery levels after the second bleach pulse would be decreased as a fraction of

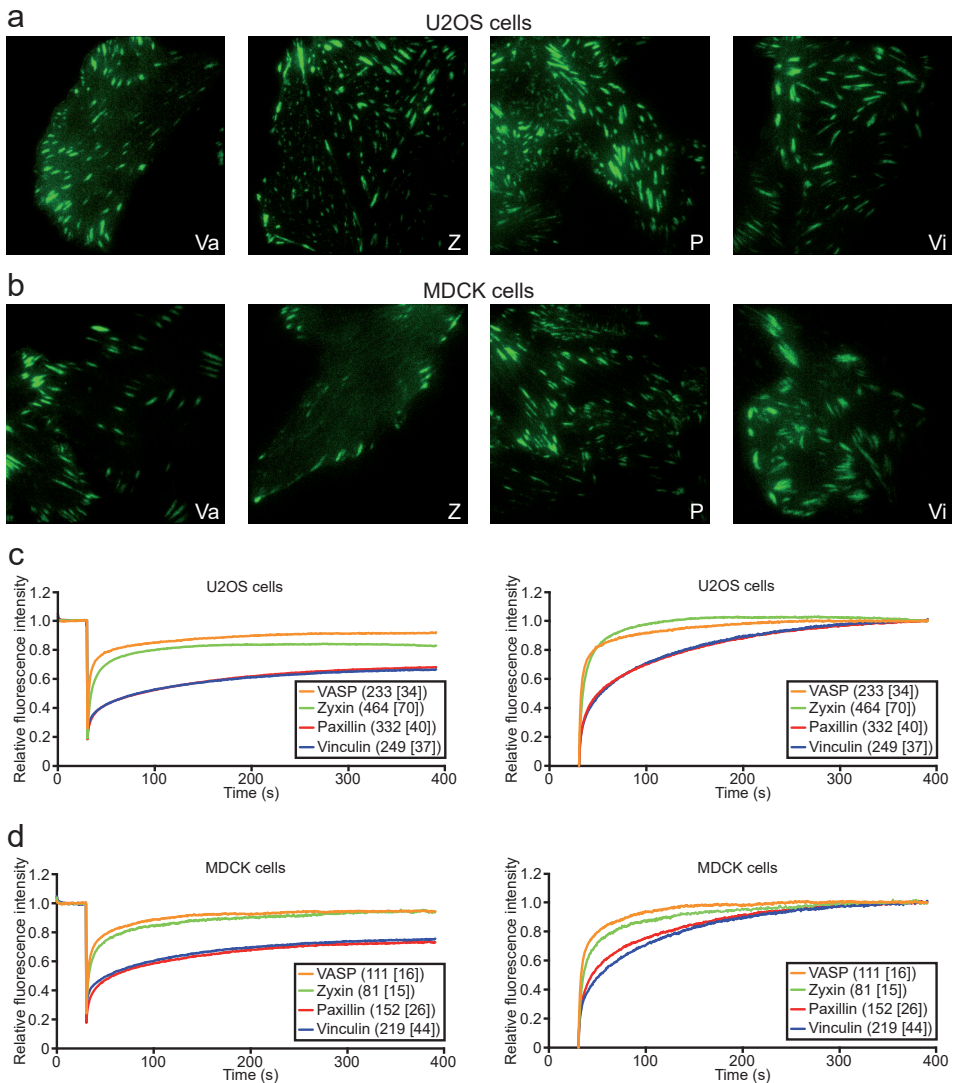


**Figure 1. Focal adhesion proteins have stably bound fractions at similar ratios across cell types.**

(a) TIRF images of the four studied proteins expressed in U2OS cells: VASP (Va), zyxin (Z), paxillin (P) and vinculin (Vi). (b) TIRF images of the four studied proteins expressed in MDCK cells. (c) FRAP-curves for U2OS cells stably expressing GFP-tagged FA proteins. In the left plot fluorescence intensity is expressed relative to prebleach levels, in the right plot relative to immediately postbleach (0) and final recovery levels (1) to facilitate comparison of the recovery rates irrespective of final recovery levels or bleach depths. The numbers between brackets indicate the number of bleached FAs from [number of cells]. (d) FRAP-curves for MDCK cells stably expressing GFP-tagged FA proteins.

the bleached proteins would exchange with other bleached proteins. However, after the second bleach pulse fluorescence recovery came to the exact same levels as after the first, demonstrating there is no significant bleaching of the fluorescent protein pool despite the fact that this control experiment contained a second

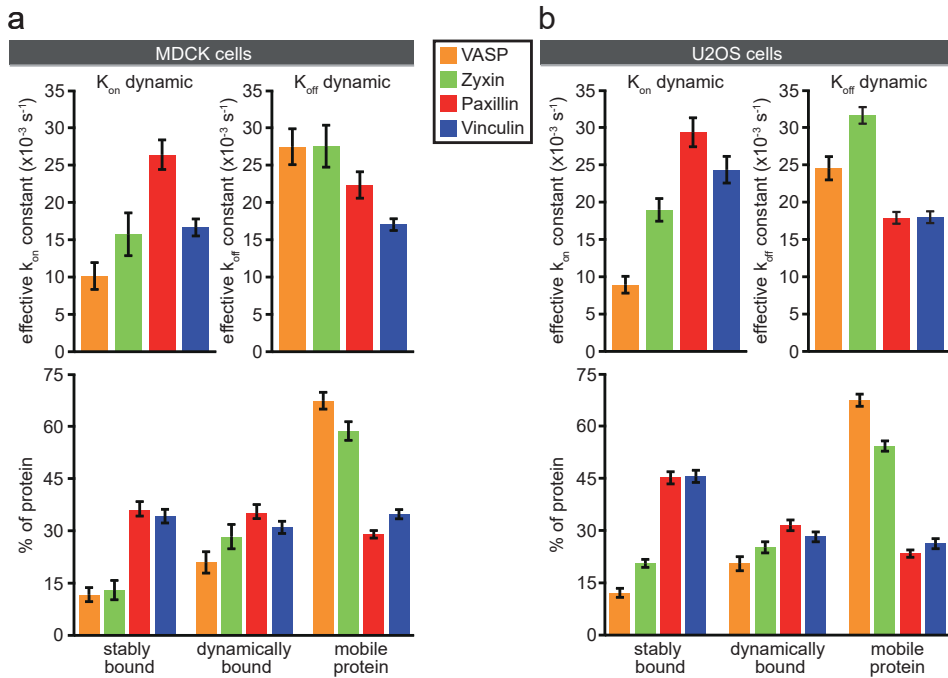


**Figure 2. Quantification of the FRAP data.**

(a) Parameters of FA protein dynamics in MDCK cells as determined by fitting the experimental curves shown in Fig. 1 to curves generated by Monte-Carlo based computer simulations. Bar charts of the effective on- and off-rate constants of the dynamically bound fractions (top panels) and the relative sizes of the stably bound, dynamically bound and mobile fractions (bottom panels). Error bars indicate  $2 \times \text{SEM}$ . VASP  $n = 111$  [16], zyxin  $n = 81$  [15], paxillin  $n = 152$  [26], vinculin  $n = 219$  [44] bleached FAs from [cells]. (b) Parameters of FA protein dynamics in U2OS cells. VASP  $n = 233$  [34], zyxin  $n = 464$  [70], paxillin  $n = 332$  [40], vinculin  $n = 249$  [37] bleached FAs from [cells].

bleach pulse. Instead, the incomplete recovery levels are due to a fraction of the protein pool being stably associated with FAs.

We quantified our data by fitting the experimentally-derived FRAP curves to curves generated by Monte Carlo based simulations<sup>41</sup> (Fig. 2). Briefly, the simulation goes through small time steps. In each step the simulated proteins, which are confined to a volume with the dimensions of a typical cell, have chances to step into a random direction, if they are freely diffusing. In addition, they have a chance to get immobilised (effective  $k_{on}$ ) when close to predefined locations (FAs). Simulated proteins bound to an FA have chances to release (effective  $k_{off}$ ). Similarly, proteins inside the laser beam during bleaching have a chance to get bleached. The simulation was systematically run with different  $k_{on}$ 's and  $k_{off}$ 's, leading to the medium and long bound fraction sizes, and their specific residence times. In this way a large database of computer generated FRAP-curves was created from which the one best fitting to the experimental data was selected. The  $k_{on}$ 's and



$k_{off}$ 's used for the best fitting simulation were used to calculate residence times and fraction sizes<sup>41</sup> (for details see Materials and Methods). The stably bound fractions obtained in this way for U2OS and [MDCK] cells are (average  $\pm$  2x SEM = Standard Error of the Mean):  $12.1 \pm 1.30$ ,  $[11.7 \pm 2.02]$ % for VASP,  $20.6 \pm 1.14$ ,  $[13.0 \pm 2.80]$ % for zyxin, and as discussed above large and of strikingly similar size for paxillin and vinculin, at  $45.1 \pm 1.74$ ,  $[36.0 \pm 2.44]$ % for paxillin and  $45.6 \pm 1.74$ ,  $[34.2 \pm 1.97]$ % for vinculin. The simulations also provide accurate estimates of the more dynamically bound fractions:  $20.5 \pm 2.05$ ,  $[20.9 \pm 3.07]$ % for VASP,  $25.2 \pm 1.61$ %,  $[28.3 \pm 3.51]$ % for zyxin  $31.5 \pm 1.54$ ,  $[35.0 \pm 2.51]$ % for paxillin and  $28.2 \pm 1.40$ ,  $[31.0 \pm 1.73]$ % for vinculin. The remainder of the protein pool was associated with FAs so briefly that its residence time was consistent with what would be expected for free diffusion. Hence, we will refer to this fraction as the mobile pool although its proteins may be very briefly immobilised at the FA complex. Additionally, fitting of the data allowed us to determine the average on- and off-rate constants for the dynamically and stably bound fractions, for the dynamic fractions these are plotted. For the stably bound fractions these did not differ significantly between the four proteins (data not shown). The average residence times of the stably bound fractions were over half an hour, which is comparable to previously reported FA lifetimes ranging from approximately 20 to 90 minutes<sup>42-44</sup>. We also examined the lifetime of 100 FAs from 5 cells in time lapse movies, which we found to be  $55 \pm 6$  (2xSEM) minutes. This indicates that a substantial part of the investigated proteins in the stably bound fractions remain associated for the entire lifetime of an FA.

## The effect of focal adhesion position and orientation on protein binding dynamics

### *Categorisation of focal adhesions based on their position and orientation*

Several factors form gradients based on their distance from the edge of the ventral membrane, such as actin fibre thickness and connectivity, the concentration of (signalling) molecules and enzyme activity<sup>33-40</sup>. Such gradients effectively create different local environments for FAs varying with their distance from the ventral membrane edge. To investigate whether such variation in local environments influences FA protein dynamics, we further subdivided the FRAP data shown in Fig. 1.

First, all FAs were grouped on the basis of their distance from the closest ventral membrane edge. 'Outer' FAs are located close to this edge, 'inner' FAs are positioned further inwards with outer FAs located between them and the closest adherent membrane edge (Fig. 3a,b).

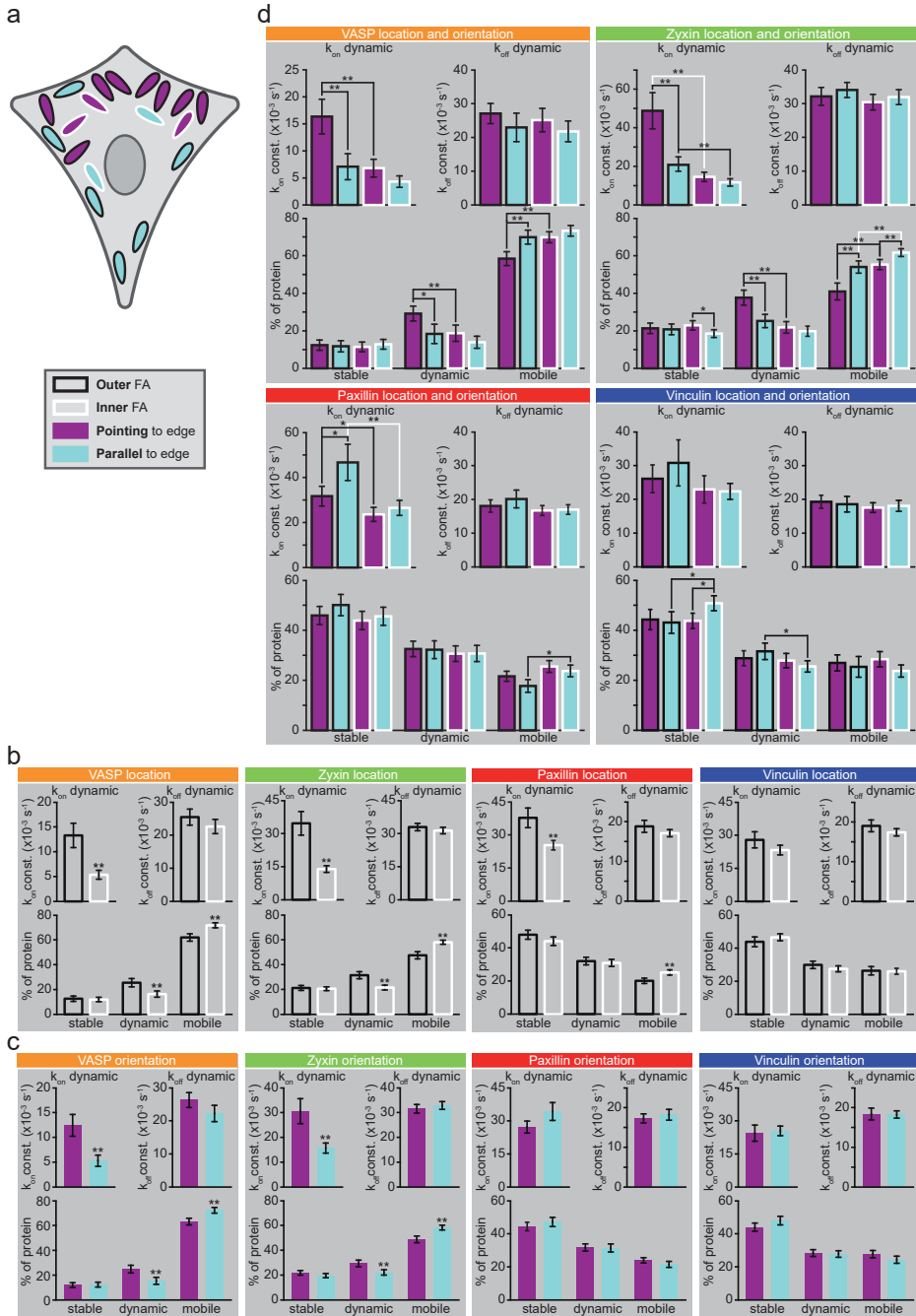


**Figure 3.** FA distance from and/or orientation relative to the closest edge of the ventral membrane influence its dynamics.

**(a)** Cartoon illustrating classification of FAs based on distance from or orientation relative to the closest edge of the ventral (adherent) portion of the plasma membrane. ‘Outer’ FAs (black outline) are

close to the edge of the ventral membrane, 'inner' FAs (white outline) are located away from the edge with outer FAs located in between. In 'pointing' FAs (purple) the longest axis is oriented more or less perpendicular to the closest membrane edge, and in 'parallel' FAs (blue) the longest axis is more or less parallel to the edge. **(b)** Quantification of U2OS cell FRAP data based on FA distance from the closest edge of the ventral membrane. VASP [34]: outer n = 100, inner n = 114, Zyxin [70]: outer n = 185, inner n = 260, Paxillin [40]: outer n = 120, inner n = 200, Vinculin [37]: outer n = 91, inner n = 158 FAs from [cells]. Error bars indicate 2xSEM. Asterisks indicate significant p-values generated by two sided Mann Whitney test: \* p < 0.01, \*\* p < 0.001 **(c)** Quantification of U2OS cell FRAP data based on FA orientation relative to the closest edge of the ventral membrane. VASP [34]: pointing n = 109, parallel n = 93, Zyxin [70]: pointing n = 199, parallel n = 209, Paxillin [40]: pointing n = 136, parallel n = 134, Vinculin [37]: pointing n = 119, parallel n = 95 FAs from [cells]. Error bars and asterisks as above. **(d)** Parameters obtained by fitting the FRAP data after categorising the FAs based on the combination of their distance from and their orientation relative to the closest edge of the ventral membrane. This is especially revealing for VASP and zyxin, as it shows that it are specifically the outer and pointing FAs that have strongly altered VASP and zyxin dynamics compared to all other FA types. N-numbers per protein for consecutively: outer and pointing, outer and parallel, inner and pointing and inner and parallel FAs: VASP: 64, 34, 45, 58, Zyxin: 90, 90, 104, 118, Paxillin: 65, 51, 67, 82, Vinculin: 56, 35, 63, 60. Error bars and asterisks as above.

In addition, we noticed that FAs are mostly orientated with their long axis either roughly perpendicular or roughly parallel to the closest adherent membrane edge. FAs were classified as 'pointing' when the angle between their long axis and the closest ventral membrane edge was  $90^\circ \pm 30^\circ$ . FAs were classified as 'parallel' when the angle between their long axis and the closest ventral membrane edge was  $180^\circ \pm 30^\circ$  (Fig. 3a,c). Of the 1278 bleached FAs (see Materials and methods for a specification per examined protein) 184 fell outside these criteria, which is 14%, whereas one third ( $60^\circ / 180^\circ$ ) would be expected if FA orientation would be random.

Finally, the adhesions were grouped based on the combination of these two criteria which results in four groups: A outer and pointing, B outer and parallel, C inner and pointing and D inner and parallel FAs (Fig. 3a,d).

#### *Differences in FA protein dynamics based on FA location*

Zyxin and VASP exchange dynamics followed the same trend when comparing outer to inner FAs (Fig. 3b). At outer FAs the on-rate constant of the dynamically associated fraction was more than twice as large, leading to a significantly increased dynamically bound fraction and a significantly decreased mobile pool.

Similarly, for paxillin the on-rate constant of the dynamically associated fraction was significantly increased at the outer FAs while the mobile pool was significantly decreased. Unlike for zyxin/VASP this last was not caused by a significant increase of the dynamically associated fraction specifically, but rather by the sum of individually insignificant increases of the dynamically and the stably associated fractions.

*Differences in FA protein dynamics based on FA orientation*

Zyxin and VASP also showed similar trends in their dynamic behaviour when comparing parallel to pointing FAs (Fig. 3c). At pointing FAs the on-rate constant of the dynamically associated fraction is more than twice as large, resulting in a significantly increased dynamically bound fraction and a significantly decreased mobile pool.

For paxillin and vinculin none of the measured parameters were significantly altered in pointing FAs compared to parallel FAs.

*Differences in FA protein dynamics based on both FA location and orientation*

Having found that FA location and orientation separately correlate to the dynamics of FA associated proteins, we next examined the four possible combinations of FA location and orientation.

Again, the dynamics of zyxin and VASP followed a similar trend, with their dynamics at the outer and pointing FAs clearly standing out from their dynamics at any other FA type (Fig. 3d). Specifically, compared to either outer and parallel or to inner and pointing FAs the size and the on-rate constants of the dynamically associated fraction was significantly increased and the mobile pool was significantly decreased. For zyxin additional significant differences in dynamic behaviour were observed when comparing the remaining FA types, however these were all of a much smaller magnitude than those seen when comparing zyxin/VASP dynamics at outer and pointing FAs to zyxin/VASP dynamics at any other FA type.

For paxillin significant differences were also observed when comparing the four different FA types, but unlike for zyxin/VASP no single FA type clearly stands out from the rest. At the outer and pointing FAs the on-rate constant of the dynamically associated fraction is decreased compared to at the outer and parallel FAs, but increased compared to at the inner and pointing FAs. At the outer and parallel FAs the on-rate of the dynamically associated fraction is increased and the mobile pool decreased compared to at the inner and parallel FAs.

Similar to the lack of correlation between vinculin dynamic behaviour and FA location or orientation separately, the combination of FA location and orientation also had little effect, but there were some significant differences. At the inner and parallel FAs the stably bound fraction was increased compared to at either the outer and parallel or the inner and pointing FAs while the dynamically associated fraction was significantly decreased compared to at the outer and parallel FAs.

## Discussion

Here we studied the dynamics of two pairs of functionally related focal adhesion proteins, paxillin/vinculin and zyxin/VASP, in two different, slow moving, non-fibroblast cell types on a collagen coating. The quantitative data were highly consistent between the cell types from different species, suggesting these findings are not cell-type specific and are relevant for FA function.

A large number of previous studies have examined the dynamics of paxillin, vinculin, zyxin or VASP in fibroblasts<sup>11,45-59</sup>, but never together in the same study. Moreover, each study used different culturing and quantitative analysis methods, leading to considerable differences in reported quantitative parameters. For instance, for paxillin, half times to full recovery were between 1.5 and 41 seconds, the times until final recovery between 30 and 200 seconds, and mobile fractions between 60% and nearly 100%. The period fibroblasts were cultured on fibronectin prior to imaging ranged from 15 minutes to 48 hours which influences spreading level, a factor known to influence the maturation of FAs, which has been shown to inhibit vinculin dynamics<sup>50</sup>. Moreover, different culturing conditions may also affect FA composition, protein phosphorylation status and conformational states and these may influence protein dynamics<sup>11,45,48-50,52,54,58</sup>. The net result of this is a large variation in the reported quantitative parameters for these FA proteins, hampering comparison with the parameters presented here, as well as the parameters for the different proteins examined in different studies. However, it may still be noted that the speed of paxillin and vinculin recovery we observed was considerably slower than in previous studies, and we found larger stably associated fractions for these proteins. Both parameters were consistent between our two different cell types, which were from different species, suggesting they are not cell-type specific and are relevant for FA function. Yet neither of the two cell types used in this study show as much or as fast unstimulated migration as fibroblasts. Thus, the slow recovery and large immobile fractions we observed might be typical of cells displaying less or slower unstimulated migration.

We demonstrated that for each of the studied proteins three different dynamic pools are present in FAs: (1) a pool with stable associations (>30 minutes), (2) a dynamically exchanging pool with shorter interactions (~1 minute) and (3) a very dynamic pool with interactions so brief that they could not be distinguished from free diffusion (referred to as the mobile pool). In both cell types the stable fraction is small for VASP, somewhat larger for zyxin and largest and surprisingly similar for paxillin and vinculin (Fig. 4a). Consistently, previous studies measuring the recovery of both paxillin and vinculin also reported highly similar immobile fractions<sup>51-54</sup>, but very different amongst studies. Since FAs show a sliding type of

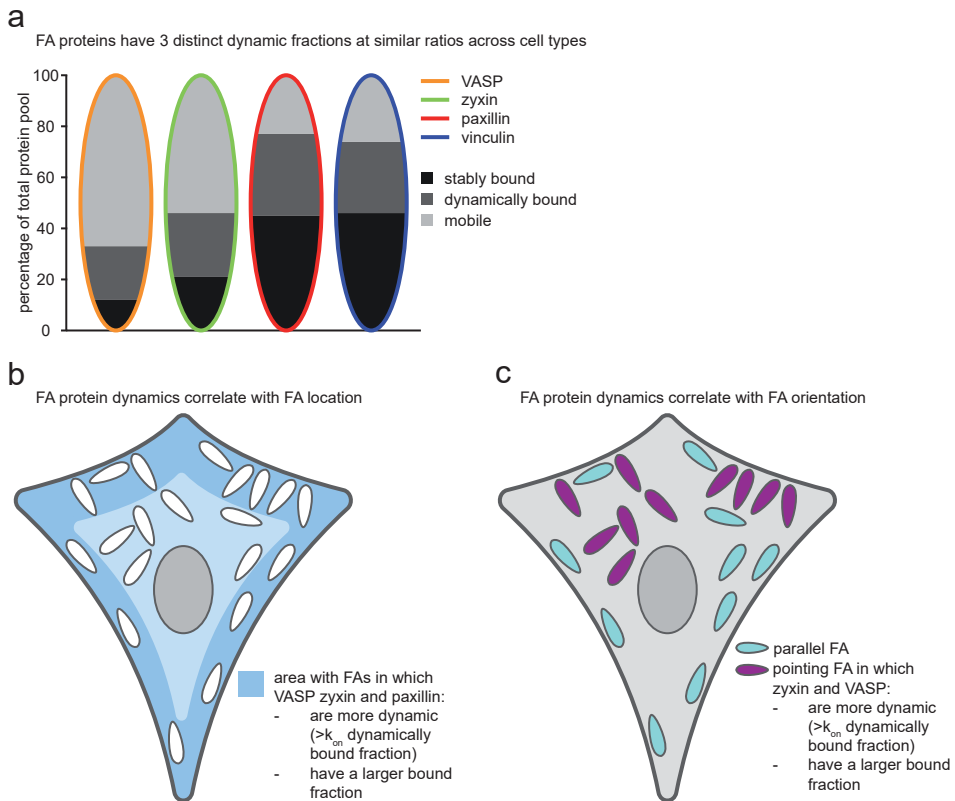


**Figure 4. Schematic overview of the data.**

(a) Model showing the ratio between the 3 dynamic fractions, stably bound, dynamically bound and mobile protein for each of the studied proteins as revealed by fitting of the experimental FRAP curves to curves generated by computer-based simulations (b) Schematic overview of how FA protein dynamics correlate with FA location, VASP, zyxin and paxillin are more dynamic (have a higher on-rate constant for the dynamically bound fraction) and a larger bound fraction at FAs located close to the ventral membrane edge. (c) Schematic overview of how FA protein dynamics correlate with FA orientation, VASP and zyxin are more dynamic (have a higher on-rate constant for the dynamically bound fraction) and a larger bound fraction at FAs orientated with their long axis more or less perpendicular to the ventral membrane edge.

movement, both in migrating and in stationary cells, they are typically regarded as highly dynamic complexes<sup>60,61</sup>. However, the average residence time of all stably associated fractions was relatively long compared to previously reported FA lifetimes and the average FA lifetime of  $55 \pm 6$  minutes observed here<sup>42-44</sup>, indicating the proteins in these fractions remain associated for a large part of the lifetime of an FA and revealing some properties of FAs are less dynamic than previously thought.

Furthermore, we show that protein binding dynamics differ with FA orientation and location relative to the closest edge of the ventral membrane (Fig. 4b,c). This

was especially true for zyxin and VASP, for which the on-rate constant of the dynamically associated fraction was more than twice as high at outer vs inner FAs and the same was true for pointing vs parallel FAs. Further investigation revealed dynamic on-rate constants were specifically increased at FAs that are outer as well as pointing. Increased on-rate constants can be the result of either increased numbers of available binding sites or of increased affinity for these sites. Because the off-rate constants of the dynamic fractions were not significantly altered, the increased on-rate constants lead to significantly increased sizes of the dynamically bound zyxin/VASP fractions at these FAs. A likely function of which is to facilitate the coupling of actin by increasing the number of available actin binding sites, as both proteins directly bind actin. Strong links between actin and FAs that lie close and perpendicular to the edge of the ventral membrane (i.e. are outer and pointing) are presumably needed to generate the force required to protrude or retract the ventral membrane. The effects of FA location and orientation on paxillin and vinculin dynamics are more subtle, for vinculin only the combination significantly correlated with its dynamics. For paxillin at outer FAs the on-rate constant of the dynamically associated fraction was significantly increased and the mobile pool significantly decreased, meaning an increased total (stable and dynamic) bound fraction. In spite of the increased on-rate constant, the dynamic fraction was not increased. This is due to the large decrease of the mobile pool, decreasing the number of paxillin molecules available for binding. With respect to biological function the increased total bound fraction of paxillin at outer FAs may be needed to deal with the increased force created by increased bound fractions of zyxin/VASP. Furthermore, an increase in the on-rate constant of the dynamically bound fraction of a structural component like paxillin, may stimulate the dynamics of the entire FA. This is supported by the increased on-rate constants of the dynamically bound VASP/zyxin fractions at outer FAs. It could be advantageous for FAs at the edge of the ventral membrane to be more dynamic when a cell is exploring its immediate environment by protruding its membrane at different areas, but is not yet committed to moving in a particular direction.

Overall it is remarkable how similar the dynamics of vinculin/paxillin are, and different from the also similar dynamics of zyxin/VASP, this last particularly with respect to the impact of FA orientation and location. The vinculin head domain and paxillin as well as zyxin/VASP share many functions and binding partners, including each other, potentially contributing to the similar binding dynamics. For the vinculin head domain and paxillin the most notable shared binding partner is talin, while zyxin/VASP both bind actin and work together in several cellular processes such as efficient cell spreading<sup>13-16,25,30-32</sup>. However,

vinculin's tail domain shares many functions and binding partners with zyxin/VASP, including zyxin/VASP themselves which depend on vinculin for many of the actin regulating processes they are involved in<sup>16-20,24-29</sup>. The remarkably similar vinculin/paxillin dynamics suggest that vinculin's head domain influences its dynamics more strongly than its tail domain. This is perhaps because vinculin, like paxillin, enters a newly forming FA complex when many of the proteins interacting with its head domain are already associated, while most of the interaction partners for its tail domain are not yet present. When at later stages the latter enter the FA complex, a large proportion of the vinculin molecules will already be extensively involved in interactions through their head domains. Later additional interactions through their tail domains will have little influence on their binding dynamics. Interestingly, in other studies looking at different aspects of protein behaviour at FAs, a split between paxillin/vinculin versus zyxin/VASP was also observed. For instance, zyxin/VASP dissociate from disassembling FAs earlier than paxillin/vinculin, including in response to actomyosin-II inhibition<sup>21,54</sup>. When stress fibres thicken, in response to mechanical stress or to the actin stabilizer jasplakinolide, VASP/zyxin rapidly translocate from FAs to the thickening stress fibres while vinculin/paxillin remain associated<sup>28,62</sup>. Zyxin is completely lost from FAs in response to actin polymerisation inhibition, while vinculin levels remain unchanged<sup>48</sup>. Overexpression of the zyxin LIM-domain causes the loss of endogenous zyxin and VASP from FAs while vinculin levels remain unchanged<sup>27,63</sup>. Thus, at FAs a distinction between paxillin/vinculin and VASP/zyxin behaviour seems to be a previously unrecognised recurring theme.

In summary, we examined the dynamics of two pairs of functionally related FA proteins, paxillin/vinculin and zyxin/VASP. For each protein we demonstrated the presence of a stably associating, a dynamically exchanging and a mobile pool within FAs. Moreover, we show there is a distinction between the dynamics of paxillin/vinculin and VASP/zyxin. A literature search revealed this distinction is a previously unrecognized but recurring theme in their behaviour at FAs. Furthermore, we show that protein binding dynamics differ with FA orientation and location. This is especially true for zyxin and VASP and most especially at FAs that are located close to the nearest ventral membrane edge and orientated with their long axis perpendicular to it. At these FAs there are significantly more zyxin and VASP proteins binding in a significantly more dynamic manner, potentially to facilitate the coupling of actin to these FAs since both proteins are directly actin-binding. The effects of FA location and orientation on paxillin and vinculin dynamics are more subtle, but it is noteworthy that at FAs close to the membrane edge paxillin binding is significantly more dynamic, presumably stimulating the dynamics of these FAs since paxillin is a key structural component. Overall, the



presented data add to unraveling and understanding the mechanisms by which FAs function in adhesion and cell migration.

## Materials and Methods

### Cell culture

MDCK cells were cultured in DMEM (Lonza) and U2OS cells in phenol-red free DMEM (Lonza) at 37 °C and 5% CO<sub>2</sub>. Culture media were supplemented with 10% FCS (Gibco), 2mM L-glutamine (Lonza), 100 U/ml Penicillin and 100 µg/ml Streptomycin (Lonza) and to maintain stable cell lines with 100 µg/ml G418. Transfections were performed using Fugene (Promega), followed by selection with G418 when creating stable cell lines. For experiments 24 mm round glass coverslips were coated overnight at 4 °C with PureCol bovine collagen type I (Advanced Biomatrix) at a final concentration of 10 µg/ml. Cells were plated onto coated coverslips 24-48 h prior to imaging.

### Constructs

The zyxin-GFP plasmid was created by replacing the mMaple3 in Zyxin-mMaple3 (Addgene101151) with eGFP from eGFP N1 (Clontech) as a BamHI NotI fragment.

The VASP-GFP, vinculin-GFP and paxillin-GFP plasmids were based on the VASP-mTurquoise (Addgene 55585), Vinculin-mTurquoise (Addgene 55587) and paxillin-mTurquoise (Addgene 55573) vectors, respectively. These use the multiple cloning site as a linker region between the protein and mTurquoise, hampering a simple colour swap. To still allow sticky-end ligation the protein, fluorescent label and empty vector backbone were all separately isolated as restriction fragments. These were ligated using sticky ends in 2 steps: (1) the protein to the fluorescent label (2) the created insert into the vector backbone. This strategy was applied to create the following constructs:

VASP-GFP: The vector backbone was isolated from paxillin-mTurquoise as an AgeI NotI fragment, VASP from VASP-mTurquoise as an AgeI BamHI fragment and GFP from eGFP N1 as a BamHI NotI fragment.

Vinculin-GFP: The vector backbone was isolated from paxillin-mTurquoise as a NheI NotI fragment, vinculin from vinculin-mTurquoise as a NheI EcoRI fragment and GFP from eGFP as an EcoRI NotI fragment.

Paxillin-GFP: The vector backbone was isolated from paxillin-mTurquoise as a BamHI NotI fragment, paxillin from paxillin-mTurquoise as a BamHI HindIII fragment and GFP from eGFP as a HindIII NotI fragment.

All constructs were checked through sequencing, one silent mutation was found (paxillin-GFP bp1461 C to G).

### **Time lapse TIRF imaging**

Time lapse movies were made for 18 hours at 10 minute intervals on a Nikon Ti-Eclipse inverted microscope equipped with a TIRF unit and a 16 bit EM CCD camera (Photometrics) in TIRF mode using a 60x 1.45NA oil immersion objective (Apochromat TIRF). Cells were maintained at 37 °C and 5% CO<sub>2</sub> using a stage-top incubator (Tokai Hit). These were used to determine the lifetimes of a 100 FAs from 5 different cells.

### **FRAP experiments**

#### *Live-cell imaging*

All FRAP data was acquired on a Nikon Ti-Eclipse inverted microscope equipped with a TIRF unit, a 3D FRAP scanning unit (Roper) and a 16 bit EM CCD camera (Photometrics) in TIRF mode and using a 60x 1.45NA oil immersion objective (Apochromat TIRF). Cells were maintained at 37 °C and 5% CO<sub>2</sub> using a stage-top incubator (Tokai Hit). Images were taken for 30 s prebleach and 6 minutes postbleach at 500 ms intervals. The FRAP unit allowed the efficient bleaching of 2 by 2 μm squares ~ 15-25 FAs spread over the field of view, which contained (portions of) several different cells, well within 300 ms. For U2OS cells the number of bleached FAs from [number of cells] were for VASP 233 [34], zyxin 464 [70], paxillin 332 [40], vinculin 249 [37] and for MDCK cells for VASP 111 [16], zyxin 81 [15], paxillin 152 [26] and vinculin 219 [44].

#### *Data analyses*

In ImageJ software<sup>64</sup> extended in the FIJI framework<sup>65</sup> ROIs were manually drawn around efficiently bleached (portions) of FAs, as well as a few unbleached FAs for control purposes and empty areas for background measurement. To control for monitor bleaching and/or bleaching of too high a proportion of the entire protein pool any experiments where the average intensity of the unbleached FAs fell below 90% of original levels were discarded. Separate experiments on MDCK cells expressing Paxillin-GFP, where the same FA was bleached a second time 4 minutes after the original bleach pulse and followed a further 4 minutes ruled out that a significant fraction of the fluorescent protein pool was bleached using our experimental setup (Supplemental Fig. S2). Data from any FAs not bleached to <20% of their average prebleach levels was excluded from analysis, as were any FAs that were not in a stable state. The resulting fluorescence intensity data was background-corrected and normalised to prebleach levels using the follow-

ing formula:

$$I_{norm} = \frac{I_t - I_{BGt}}{I_{pre} - I_{BGpre}}$$

Where  $I_{norm}$  is the normalised FA intensity,  $I_t$  is the raw intensity of the FA at time point  $t$  and  $I_{pre}$  is the average raw intensity of the FA during the entire prebleach period,  $I_{BGt}$  and  $I_{BGpre}$  are the corresponding intensities of the average background signal for the experiment.

To facilitate comparison of the recovery rates for the different proteins irrespective of their final recovery levels the data was also normalised in such a way as to set the first value after bleaching to zero and the final recovery level to 1 using the following formula:

$$I_{norm} = \frac{(I_t - I_{BGt}) - (I_0 - I_{BG0})}{(I_{post} - I_{BGpost}) - (I_0 - I_{BG0})}$$

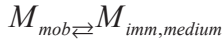
Where  $I_{norm}$  is the normalised FA intensity,  $I_t$  is the raw intensity of the FA at time point  $t$ ,  $I_0$  at the first time point after bleaching and  $I_{post}$  the average raw intensity of the FA during the last 25 time points of the experiment,  $I_{BGt}$ ,  $I_{BG0}$  and  $I_{BGpost}$  are the corresponding average background signals for the experiment.

#### *Fitting of the experimentally derived FRAP curves using Monte-Carlo based simulations*

For analysis of FRAP data, FRAP curves were normalized to prebleach values. A database of Monte Carlo based computer simulated FRAP curves was generated in which four parameters representing mobility properties were varied: long and medium immobile fractions (random values between 0% and 70%) and time spent in immobile state, ranging from medium residence times (random values between 20 and 100 s) to long residence times (random values between 600 and 3200 s). Database sizes of 5122/2027 simulated FRAP curves were used for the analysis of the FRAP data from the U2OS or MDCK cells respectively. The simulated curves are based on a model of diffusion in an ellipsoid volume representing the cell with ellipsoid volumes representing FAs and simple binding kinetics representing binding to the FA complex. Simulations were performed at unit time steps of 100 ms. Results of the simulation were evaluated every 500 ms corresponding to the experimental sample rate. The diffusion coefficient of  $1 \mu\text{m}^2/\text{s}$  was based on separate experiments measuring free diffusion of paxillin-GFP in the cytoplasm. Diffusion was simulated by deriving novel positions  $(x_{t+\Delta t}, y_{t+\Delta t}, z_{t+\Delta t})$  at each time step  $t+\Delta t$  for all mobile molecules from their current positions  $(x_t, y_t, z_t)$  by  $x_{t+\Delta t} = x_t + G(r_1)$ ,  $y_{t+\Delta t} = y_t + G(r_2)$ , and  $z_{t+\Delta t} = z_t + G(r_3)$ , where  $r_i$

is a random number ( $0 \leq r_i \leq 1$ ) chosen from a uniform distribution, and  $G(r_i)$  is an inverse cumulative Gaussian distribution with  $\mu = 0$  and  $\sigma^2 = 2Dt$ , where  $D$  is the diffusion coefficient and  $t$  is time measured in unit time steps.

Immobilisation in FAs was based on simple binding kinetics with two immobile fractions, a medium and a long fraction:



Where  $M_{mob}$  are the mobile molecules and  $M_{imm,medium}$  and  $M_{imm,long}$  are the molecules in the medium and the long immobile fractions respectively.

Each mobile molecule in the simulation can bind at the adhesion for a medium length of time with a given chance. Once a molecule becomes a part of the medium immobile fraction it has a chance to either become mobile again or to become a part of the long immobile fraction. Molecules in the long immobile fraction have a chance of becoming mobile again. These chances are defined in accordance with the following kinetics described by:

$$k_{off} = \frac{1}{t_r}$$

Where  $k_{off}$  is the off rate constant in  $s^{-1}$  for the medium or the long immobile fraction and  $t_r$  is the average time in s spent immobile for molecules in this fraction.

$$k_{on,medium} = \frac{F_{imm,medium}}{1 - F_{imm,medium} - F_{imm,long}} \cdot (k_{off,medium} + k_{on,long})$$

Where  $k_{on,medium}$  and  $k_{on,long}$  are the effective on rate constants in  $s^{-1}$  for the medium/long immobile fractions and  $F_{imm,medium}/F_{imm,long}$  are the relative number of medium/long immobile molecules respectively.

$$k_{on,long} = \frac{F_{imm,long}}{F_{imm,medium}} \cdot k_{off,long}$$

The ellipsoid volume of the cell was based on experimentally derived estimates of cell size, for U2OS cells this corresponds to a width of 24  $\mu m$ , a length of 44  $\mu m$  and a height of 2  $\mu m$ , for MDCK to 15, 64 and 2  $\mu m$  respectively. In each cell 2 ellipsoid volumes with widths of 1.5  $\mu m$ , lengths of 2  $\mu m$  and heights of 0.5  $\mu m$

were used to simulate FAs

The FRAP procedure was simulated on the basis of an experimentally derived 3D laser intensity profile providing a chance for each molecule to be bleached, based on its 3D position, during simulation of the bleach pulse. The number of fluorescent molecules in the ellipsoid volume of the bleached adhesion was used as the output of the simulation.

The experimentally derived FRAP curve for each individual FA was individually fitted to the simulated FRAP curves and the best fitting (least squares) curve was determined. For the parameters of interest,  $k_{on,medium}$  and  $k_{off,medium}$  we determined the interquartile range (IQR). Any FAs for which the best fitting curve resulted in a  $k_{on,medium}$  or  $k_{off,medium}$  outside of  $1.5 \cdot \text{IQR}$ , the next best fitting curve was used iteratively until the parameter fell within  $1.5 \cdot \text{IQR}$  range.

To give the resultant kinetic parameters for a set of FAs of interest the average was taken of the parameters corresponding to the best fitting curves for these FAs.

## Classification of FAs

To examine the effects of FA location and/or orientation all FAs were classified. FAs were classified as 'outer' when they were located close to the ventral (adherent) membrane edge. FAs were classified as 'inner' when they were located further inwards, with another FA located between them and the closest membrane edge. FAs were classified as 'pointing' when they were orientated with their long axis 'perpendicular' (*i.e.*  $90^\circ \pm 30^\circ$ ) to the closest ventral membrane edge. FAs were classified as 'parallel' when they were orientated with their long axis 'parallel' (*i.e.*  $180^\circ \pm 30^\circ$ ) to the closest membrane edge. FAs outside these boundaries were discarded in these analyses, which for the FRAP data amounted to 31 of 233 FA for VASP (13%), 56 of 464 FAs for zyxin (12%), 62 of 332 FAs for paxillin (19%) and 35 of 249 FAs for vinculin (14%). Overall, from the FRAP data 184 of the 1278 bleached FAs (14%) fell outside the criteria for 'pointing' and 'parallel' and were discarded from analyses looking at FA orientation.

## Statistical analysis

For analyses of the differences between two groups two-tailed Mann-Whitney  $U$  tests were used. For analyses of the differences between more than two groups two-tailed Kruskal-Wallis Rank Sum tests were used, if this generated a  $p$ -value  $< 0.05$  the specific groups with significant differences were determined using two-tailed Mann-Whitney  $U$  tests. To curtail the number of Mann-Whitney  $U$  tests to be performed on the FRAP data separated based on FA location and orientation

into four groups only the differences between meaningful combinations were analysed limiting the number of tests to 4 per parameter: outer pointing versus inner pointing, outer parallel versus inner parallel, outer pointing versus outer parallel and inner pointing versus inner parallel. As a further precaution against an inflated type I error rate, for all FRAP data where the FAs were separated on the basis of FA location and/or orientation the p-value was adjusted to  $< 0.01$  to denote significance

## Acknowledgements

We thank drs E Spanjaard and J. de Rooij for discussion and providing cell lines.

## Author contributions

K.L. designed and performed microscopy experiments and wrote the manuscript; B.G. designed FRAP analysis software and performed the analyses; A.B.H. supervised the project, contributed to method and analysis development, supervised writing the manuscript and revised it.

## References

- 1 Yamada, K. M. & Geiger, B. Molecular interactions in cell adhesion complexes. *Current opinion in cell biology* 9, 76-85 (1997).
- 2 Geiger, B., Bershadsky, A., Pankov, R. & Yamada, K. M. Transmembrane crosstalk between the extracellular matrix--cytoskeleton crosstalk. *Nature reviews. Molecular cell biology* 2, 793-805, doi:10.1038/35099066 (2001).
- 3 Zaidel-Bar, R., Itzkovitz, S., Ma'ayan, A., Iyengar, R. & Geiger, B. Functional atlas of the integrin adhesome. *Nature cell biology* 9, 858-867, doi:10.1038/ncb0807-858 (2007).
- 4 Winograd-Katz, S. E., Fassler, R., Geiger, B. & Legate, K. R. The integrin adhesome: from genes and proteins to human disease. *Nature reviews. Molecular cell biology* 15, 273-288, doi:10.1038/nrm3769 (2014).
- 5 Wahl, S. M., Feldman, G. M. & McCarthy, J. B. Regulation of leukocyte adhesion and signaling in inflammation and disease. *Journal of leukocyte biology* 59, 789-796 (1996).
- 6 Maartens, A. P. & Brown, N. H. The many faces of cell adhesion during *Drosophila* muscle development. *Developmental biology* 401, 62-74, doi:10.1016/j.ydbio.2014.12.038 (2015).
- 7 Laukaitis, C. M., Webb, D. J., Donais, K. & Horwitz, A. F. Differential dynamics of alpha 5 integrin, paxillin, and alpha-actinin during formation and disassembly of adhesions in migrating cells. *The Journal of cell biology* 153, 1427-1440 (2001).
- 8 Webb, D. J. et al. FAK-Src signalling through paxillin, ERK and MLCK regulates adhesion disassembly. *Nature cell biology* 6, 154-161, doi:10.1038/ncb1094 (2004).
- 9 Wiseman, P. W. et al. Spatial mapping of integrin interactions and dynamics during cell migration by image correlation microscopy. *Journal of cell science* 117, 5521-5534, doi:10.1242/jcs.01416 (2004).
- 10 Choi, C. K. et al. Actin and alpha-actinin orchestrate the assembly and maturation of nascent adhesions in a myosin II motor-independent manner. *Nature cell biology* 10, 1039-1050, doi:10.1038/ncb1763 (2008).

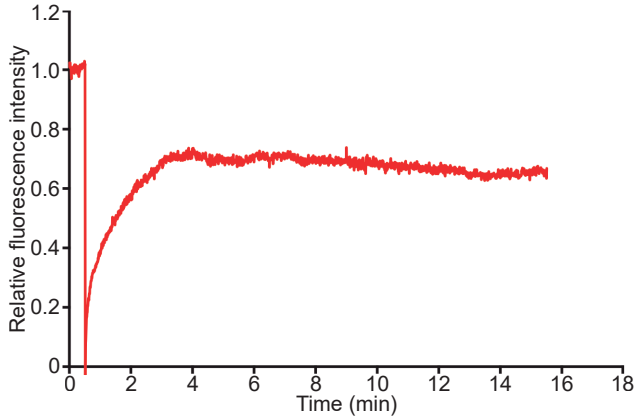
- 11 Pasapera, A. M., Schneider, I. C., Rericha, E., Schlaepfer, D. D. & Waterman, C. M. Myosin II activity regulates vinculin recruitment to focal adhesions through FAK-mediated paxillin phosphorylation. *The Journal of cell biology* 188, 877-890, doi:10.1083/jcb.200906012 (2010).
- 12 Bakolitsa, C. et al. Structural basis for vinculin activation at sites of cell adhesion. *Nature* 430, 583-586, doi:10.1038/nature02610 (2004).
- 13 Jones, P. et al. Identification of a talin binding site in the cytoskeletal protein vinculin. *The Journal of cell biology* 109, 2917-2927 (1989).
- 14 Turner, C. E. & Miller, J. T. Primary sequence of paxillin contains putative SH2 and SH3 domain binding motifs and multiple LIM domains: identification of a vinculin and pp125Fak-binding region. *Journal of cell science* 107 ( Pt 6), 1583-1591 (1994).
- 15 Brown, M. C., Perrotta, J. A. & Turner, C. E. Identification of LIM3 as the principal determinant of paxillin focal adhesion localization and characterization of a novel motif on paxillin directing vinculin and focal adhesion kinase binding. *The Journal of cell biology* 135, 1109-1123 (1996).
- 16 Humphries, J. D. et al. Vinculin controls focal adhesion formation by direct interactions with talin and actin. *The Journal of cell biology* 179, 1043-1057, doi:10.1083/jcb.200703036 (2007).
- 17 McGregor, A., Blanchard, A. D., Rowe, A. J. & Critchley, D. R. Identification of the vinculin-binding site in the cytoskeletal protein alpha-actinin. *The Biochemical journal* 301 ( Pt 1), 225-233 (1994).
- 18 Brindle, N. P., Holt, M. R., Davies, J. E., Price, C. J. & Critchley, D. R. The focal-adhesion vasodilator-stimulated phosphoprotein (VASP) binds to the proline-rich domain in vinculin. *The Biochemical journal* 318 ( Pt 3), 753-757 (1996).
- 19 Gertler, F. B., Niebuhr, K., Reinhard, M., Wehland, J. & Soriano, P. Mena, a relative of VASP and *Drosophila Enabled*, is implicated in the control of microfilament dynamics. *Cell* 87, 227-239 (1996).
- 20 Reinhard, M., Rudiger, M., Jockusch, B. M. & Walter, U. VASP interaction with vinculin: a recurring theme of interactions with proline-rich motifs. *FEBS letters* 399, 103-107 (1996).
- 21 Rottner, K., Krause, M., Gimona, M., Small, J. V. & Wehland, J. Zyxin is not colocalized with vasodilator-stimulated phosphoprotein (VASP) at lamellipodial tips and exhibits different dynamics to vinculin, paxillin, and VASP in focal adhesions. *Molecular biology of the cell* 12, 3103-3113 (2001).
- 22 Furman, C. et al. Ena/VASP is required for endothelial barrier function in vivo. *The Journal of cell biology* 179, 761-775, doi:10.1083/jcb.200705002 (2007).
- 23 Hirata, H., Tatsumi, H. & Sokabe, M. Zyxin emerges as a key player in the mechanotransduction at cell adhesive structures. *Communicative & integrative biology* 1, 192-195 (2008).
- 24 Golsteyn, R. M., Beckerle, M. C., Koay, T. & Friederich, E. Structural and functional similarities between the human cytoskeletal protein zyxin and the ActA protein of *Listeria monocytogenes*. *Journal of cell science* 110 ( Pt 16), 1893-1906 (1997).
- 25 Drees, B. et al. Characterization of the interaction between zyxin and members of the Ena/vasodilator-stimulated phosphoprotein family of proteins. *The Journal of biological chemistry* 275, 22503-22511, doi:10.1074/jbc.M001698200 (2000).
- 26 Fradelizi, J. et al. ActA and human zyxin harbour Arp2/3-independent actin-polymerization activity. *Nature cell biology* 3, 699-707, doi:10.1038/35087009 (2001).
- 27 Nix, D. A. et al. Targeting of zyxin to sites of actin membrane interaction and to the nucleus. *The Journal of biological chemistry* 276, 34759-34767, doi:10.1074/jbc.M102820200 (2001).
- 28 Yoshigi, M., Hoffman, L. M., Jensen, C. C., Yost, H. J. & Beckerle, M. C. Mechanical force mobilizes zyxin from focal adhesions to actin filaments and regulates cytoskeletal reinforcement. *The Journal of cell biology* 171, 209-215, doi:10.1083/jcb.200505018 (2005).
- 29 Hoffman, L. M. et al. Genetic ablation of zyxin causes Mena/VASP mislocalization, increased motility, and deficits in actin remodeling. *The Journal of cell biology* 172, 771-782, doi:10.1083/jcb.200512115 (2006).

- 30 Hoffman, L. M. et al. Targeted disruption of the murine zyxin gene. *Molecular and cellular biology* 23, 70-79 (2003).
- 31 Smith, M. A. et al. A zyxin-mediated mechanism for actin stress fiber maintenance and repair. *Developmental cell* 19, 365-376, doi:10.1016/j.devcel.2010.08.008 (2010).
- 32 Uemura, A., Nguyen, T. N., Steele, A. N. & Yamada, S. The LIM domain of zyxin is sufficient for force-induced accumulation of zyxin during cell migration. *Biophysical journal* 101, 1069-1075, doi:10.1016/j.bpj.2011.08.001 (2011).
- 33 Barsony, J. & Marx, S. J. Immunocytology on microwave-fixed cells reveals rapid and agonist-specific changes in subcellular accumulation patterns for cAMP or cGMP. *Proceedings of the National Academy of Sciences of the United States of America* 87, 1188-1192 (1990).
- 34 Neher, E. & Augustine, G. J. Calcium gradients and buffers in bovine chromaffin cells. *The Journal of physiology* 450, 273-301 (1992).
- 35 Ponti, A., Machacek, M., Gupton, S. L., Waterman-Storer, C. M. & Danuser, G. Two distinct actin networks drive the protrusion of migrating cells. *Science (New York, N.Y.)* 305, 1782-1786, doi:10.1126/science.1100533 (2004).
- 36 Nikolaev, V. O., Bunemann, M., Schmitteckert, E., Lohse, M. J. & Engelhardt, S. Cyclic AMP imaging in adult cardiac myocytes reveals far-reaching beta1-adrenergic but locally confined beta2-adrenergic receptor-mediated signaling. *Circulation research* 99, 1084-1091, doi:10.1161/01.RES.0000250046.69918.d5 (2006).
- 37 Lynch, M. J., Baillie, G. S. & Houslay, M. D. cAMP-specific phosphodiesterase-4D5 (PD-E4D5) provides a paradigm for understanding the unique non-redundant roles that PDE4 isoforms play in shaping compartmentalized cAMP cell signalling. *Biochemical Society transactions* 35, 938-941, doi:10.1042/bst0350938 (2007).
- 38 Dixit, N. & Simon, S. I. Chemokines, selectins and intracellular calcium flux: temporal and spatial cues for leukocyte arrest. *Frontiers in immunology* 3, 188, doi:10.3389/fimmu.2012.00188 (2012).
- 39 Mehta, S. et al. Calmodulin-controlled spatial decoding of oscillatory Ca<sup>2+</sup> signals by calcineurin. *eLife* 3, e03765, doi:10.7554/eLife.03765 (2014).
- 40 van Unen, J. et al. Plasma membrane restricted RhoGEF activity is sufficient for RhoA-mediated actin polymerization. *Scientific reports* 5, 14693, doi:10.1038/srep14693 (2015).
- 41 Geverts, B., van Royen, M. E. & Houtsmuller, A. B. Analysis of biomolecular dynamics by FRAP and computer simulation. *Methods in molecular biology (Clifton, N.J.)* 1251, 109-133, doi:10.1007/978-1-4939-2080-8\_7 (2015).
- 42 Ren, X. D. et al. Focal adhesion kinase suppresses Rho activity to promote focal adhesion turnover. *Journal of cell science* 113 ( Pt 20), 3673-3678 (2000).
- 43 Gupton, S. L. & Waterman-Storer, C. M. Spatiotemporal feedback between actomyosin and focal-adhesion systems optimizes rapid cell migration. *Cell* 125, 1361-1374, doi:10.1016/j.cell.2006.05.029 (2006).
- 44 Zaidel-Bar, R., Milo, R., Kam, Z. & Geiger, B. A paxillin tyrosine phosphorylation switch regulates the assembly and form of cell-matrix adhesions. *Journal of cell science* 120, 137-148, doi:10.1242/jcs.03314 (2007).
- 45 von Wichert, G., Haimovich, B., Feng, G. S. & Sheetz, M. P. Force-dependent integrin-cytoskeleton linkage formation requires downregulation of focal complex dynamics by Shp2. *The EMBO journal* 22, 5023-5035, doi:10.1093/emboj/cdg492 (2003).
- 46 Chandrasekar, I. et al. Vinculin acts as a sensor in lipid regulation of adhesion-site turnover. *Journal of cell science* 118, 1461-1472, doi:10.1242/jcs.01734 (2005).
- 47 Cohen, D. M., Kutscher, B., Chen, H., Murphy, D. B. & Craig, S. W. A conformational switch in vinculin drives formation and dynamics of a talin-vinculin complex at focal adhesions. *The Journal of biological chemistry* 281, 16006-16015, doi:10.1074/jbc.M600738200 (2006).
- 48 Lele, T. P. et al. Mechanical forces alter zyxin unbinding kinetics within focal adhesions of



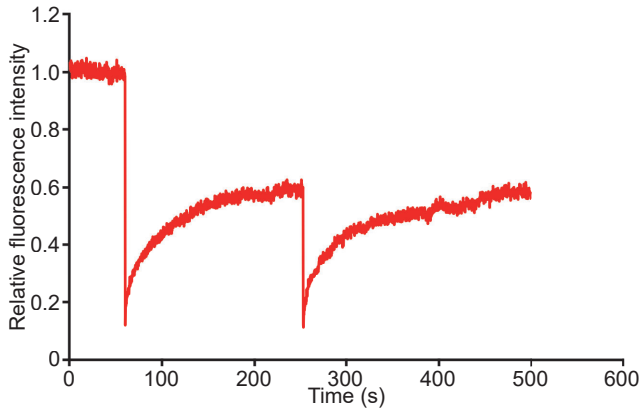
- living cells. *Journal of cellular physiology* 207, 187-194, doi:10.1002/jcp.20550 (2006).
- 49 Lele, T. P., Thodeti, C. K., Pendse, J. & Ingber, D. E. Investigating complexity of protein-protein interactions in focal adhesions. *Biochemical and biophysical research communications* 369, 929-934, doi:10.1016/j.bbrc.2008.02.137 (2008).
- 50 Mohl, C. et al. Becoming stable and strong: the interplay between vinculin exchange dynamics and adhesion strength during adhesion site maturation. *Cell motility and the cytoskeleton* 66, 350-364, doi:10.1002/cm.20375 (2009).
- 51 Wolfenson, H. et al. A role for the juxtamembrane cytoplasm in the molecular dynamics of focal adhesions. *PLoS one* 4, e4304, doi:10.1371/journal.pone.0004304 (2009).
- 52 Horton, E. R. et al. Modulation of FAK and Src adhesion signaling occurs independently of adhesion complex composition. *The Journal of cell biology* 212, 349-364, doi:10.1083/jcb.201508080 (2016).
- 53 Wolfenson, H., Bershadsky, A., Henis, Y. I. & Geiger, B. Actomyosin-generated tension controls the molecular kinetics of focal adhesions. *Journal of cell science* 124, 1425-1432, doi:10.1242/jcs.077388 (2011).
- 54 Lavelin, I. et al. Differential effect of actomyosin relaxation on the dynamic properties of focal adhesion proteins. *PLoS one* 8, e73549, doi:10.1371/journal.pone.0073549 (2013).
- 55 Schiefermeier, N. et al. The late endosomal p14-MP1 (LAMTOR2/3) complex regulates focal adhesion dynamics during cell migration. *The Journal of cell biology* 205, 525-540, doi:10.1083/jcb.201310043 (2014).
- 56 Feutlinske, F. et al. Stonin1 mediates endocytosis of the proteoglycan NG2 and regulates focal adhesion dynamics and cell motility. *Nature communications* 6, 8535, doi:10.1038/ncomms9535 (2015).
- 57 Doyle, A. D., Carvajal, N., Jin, A., Matsumoto, K. & Yamada, K. M. Local 3D matrix micro-environment regulates cell migration through spatiotemporal dynamics of contractility-dependent adhesions. *Nature communications* 6, 8720, doi:10.1038/ncomms9720 (2015).
- 58 Sathe, A. R., Shivashankar, G. V. & Sheetz, M. P. Nuclear transport of paxillin depends on focal adhesion dynamics and FAT domains. *Journal of cell science* 129, 1981-1988, doi:10.1242/jcs.172643 (2016).
- 59 Le Devedec, S. E. et al. The residence time of focal adhesion kinase (FAK) and paxillin at focal adhesions in renal epithelial cells is determined by adhesion size, strength and life cycle status. *Journal of cell science* 125, 4498-4506, doi:10.1242/jcs.104273 (2012).
- 60 Smilenov, L. B., Mikhailov, A., Pelham, R. J., Marcantonio, E. E. & Gundersen, G. G. Focal adhesion motility revealed in stationary fibroblasts. *Science (New York, N.Y.)* 286, 1172-1174 (1999).
- 61 Zamir, E. et al. Dynamics and segregation of cell-matrix adhesions in cultured fibroblasts. *Nature cell biology* 2, 191-196, doi:10.1038/35008607 (2000).
- 62 Bubb, M. R., Spector, I., Beyer, B. B. & Fosen, K. M. Effects of jasplakinolide on the kinetics of actin polymerization. An explanation for certain in vivo observations. *The Journal of biological chemistry* 275, 5163-5170 (2000).
- 63 Hirata, H., Tatsumi, H. & Sokabe, M. Mechanical forces facilitate actin polymerization at focal adhesions in a zyxin-dependent manner. *Journal of cell science* 121, 2795-2804, doi:10.1242/jcs.030320 (2008).
- 64 Schneider, C. A., Rasband, W. S. & Eliceiri, K. W. NIH Image to ImageJ: 25 years of image analysis. *Nature methods* 9, 671-675 (2012).
- 65 Schindelin, J. et al. Fiji: an open-source platform for biological-image analysis. *Nature methods* 9, 676-682, doi:10.1038/nmeth.2019 (2012).

## Supplementary Figures

**S1**

**Supplementary Figure S1. Prolonged FRAP applied to paxillin in MDCK cells.**

Fluorescence intensity of paxillin-GFP expressed relative to prebleach levels and intensity immediately after the bleach pulse.

**S2**

**Supplementary Figure S2. Repeated FRAP applied to paxillin in MDCK cells.**

Fluorescence intensity of paxillin-GFP expressed relative to prebleach levels. The bleach pulse was repeated after 3.5 minutes.





# Appendix

Summary

Samenvatting

Scientific publications

Curriculum Vitae

PhD portfolio

Dankwoord

## Summary

In multicellular organisms, different cells are organised together into tissues. A large three-dimensional network of proteins and sugars, the extracellular matrix (ECM), surrounds the cells in a tissue and provides additional structural support. To ensure tissue integrity it is important that most cells remain fixed in place. For this purpose, cells attach to each other as well as to the ECM. The attachment of cells to the ECM is mediated primarily by focal adhesions (FAs), complexes of up to hundreds of different bound proteins. In this thesis focal adhesions were studied using different advanced microscopy techniques, with all techniques providing different forms of information about these complex structures.

In **chapter 1** the role of focal adhesions in biology is discussed. They are especially important for processes in which cell migration plays a major role, such as embryonic development, the functioning of the immune system or metastasis of cancer cells. Furthermore, the main molecular components of focal adhesions are discussed, with special attention to the four FA proteins specifically examined in this thesis, paxillin, vinculin, zyxin and VASP. Finally, the advanced fluorescence microscopy techniques applied in the different chapters are introduced.

In **chapter 2** FA protein dynamics was studied using Fluorescence Recovery After Photobleaching (FRAP). Here, fluorescent (luminescent) proteins were coupled to the four selected FA proteins. Since FA proteins bind to and accumulate in focal adhesions, these also become fluorescent. The fluorescence of FAs was followed over time and plotted in FRAP curves. A number of focal adhesions were exposed to a bleach pulse. This laser pulse is powerful enough to destroy (bleach) fluorescent proteins, causing the FRAP curve to drop sharply. Fluorescence will increase again if the bleached proteins are able to exchange with other, unbleached, proteins. Analysis of FRAP curves showed that the dynamics of paxillin and vinculin in focal adhesions were surprisingly stable and similar, even in two different cell types from different species. Almost half of the paxillin and vinculin proteins bound in focal adhesions were stably bound with binding times comparable to the average FA lifetime. Zyxin and VASP were more dynamically associated with focal adhesions. In addition, we showed that the binding dynamics of FA proteins correlated with focal adhesion location and orientation. In focal adhesions close to the edge of the adherent cell membrane, paxillin, zyxin and VASP were more dynamically bound and had larger bound fractions than in FAs located further from this edge. Zyxin and VASP were also more dynamically bound and had larger bound fractions in FAs that were perpendicular to this membrane edge than in focal adhesions orientated parallel to it. The increased dynamics of an important structural protein such as paxillin, like in focal adhe-



sions close to the membrane edge, might increase the dynamics of the entire focal adhesion. A larger bound fraction of the actin-binding proteins zyxin and VASP potentially enhances actin coupling to the FAs in question.

In **chapter 3** a dedicated photoconversion assay to specifically visualise stably bound proteins within subcellular structures or organelles was developed. We successfully applied this technique to further investigate the large stably bound fractions of paxillin and vinculin in focal adhesions. This showed that, although paxillin and vinculin were uniformly distributed over FAs, the stable bound paxillin and vinculin proteins formed small clusters within focal adhesions. These clusters were much smaller for paxillin than for vinculin. This means that the stably bound paxillin proteins concentrated more strongly, since we showed in chapter 2 that the stably bound fractions of paxillin and vinculin are almost the same size. In addition, the stably bound protein clusters were significantly more likely to be at the focal adhesion half furthest from the adherent membrane edge. The actin fibre also enters the FA from this side. The effects of FA orientation and location appeared to be more subtle on the stably bound protein clusters than on FA protein binding dynamics, however the surface area of the stably bound vinculin clusters was significantly increased at parallel FAs close to the membrane edge compared to parallel FAs further away from this edge.

In **chapter 4** the distribution of the selected FA proteins along the long axis of focal adhesions was studied using the superresolution technique structured illumination microscopy. At the FA end closest to the edge of the adherent membrane ('head'), paxillin protruded further than the other three proteins. At the opposite FA end ('tail'), vinculin, zyxin and VASP protruded, with vinculin protruding the furthest. When cells were stimulated with HGF, the paxillin heads became shorter and the zyxin tails longer. In addition, focal adhesions at protruding or retracting membrane edges had longer paxillin heads than focal adhesions at static membrane edges. Taken together, this suggests movement influences the distribution of FA proteins along focal adhesions

Finally, in **chapter 5** the coupling between focal adhesions and actin was studied in detail, using a technique combining fluorescence microscopy and electron microscopy in a single microscope. This revealed that, for nearly all focal adhesions, the actin fibre entry site was darker in the electron microscopy images. This locally increased contrast indicates a higher protein density, possibly in combination with increased protein phosphorylation levels. In nearly three quarters of the focal adhesions, these areas of increased contrast had a forked nanostructure, with the actin fibre forming the stem of the fork and the focal adhesion areas with increased contrast forming the fork.

## Samenvatting

In meercellige organismen zijn verschillende cellen samen gegroepeerd en georganiseerd als weefsels. Een groot driedimensionaal netwerk van eiwitten en suikers, de extracellulaire matrix (ECM), omgeeft de cellen van weefsels en voegt zo structurele ondersteuning toe. Om de weefselintegriteit te kunnen garanderen is het belangrijk dat de meeste cellen op hun plaats blijven. Daartoe hechten cellen zowel aan elkaar als aan de ECM. Het hechten van cellen aan de ECM gebeurt voornamelijk via focale adhesies (FA's), complexen van tot honderden verschillende aan elkaar gebonden eiwitten. In dit proefschrift zijn focale adhesies met verschillende geavanceerde microscopie technieken bestudeerd, waarbij alle technieken andere informatie over deze complexe structuren verschaffen.

In **hoofdstuk 1** wordt de rol van focale adhesies binnen de biologie besproken. Ze zijn vooral van belang voor processen waarbij celmigratie een grote rol speelt, zoals de embryonale ontwikkeling, het functioneren van het immuunsysteem of het uitzaaien van kankercellen. Verder wordt er ingegaan op de belangrijkste moleculaire componenten van focale adhesies, met speciale aandacht voor de vier FA-eiwitten die in dit proefschrift specifiek worden bekeken, paxillin, vinculin, zyxin en VASP. Tenslotte worden de geavanceerde fluorescentie microscopie technieken die in de verschillende hoofdstukken zijn toegepast geïntroduceerd.

In **hoofdstuk 2** werd de dynamiek van FA eiwitten bestudeerd door middel van Fluorescence Recovery After Photobleaching (FRAP). Hiervoor werden fluorescente (lichtgevende) eiwitten aan de vier geselecteerde FA-eiwitten gekoppeld. Doordat de FA-eiwitten binden en zich ophopen in focale adhesies werden deze hierdoor ook fluorescent. De fluorescentie van FA's werd gevolgd door de tijd en uitgezet in een grafiek, de FRAP-curve. Een aantal FA's werd belicht met een bleekpuls. Deze laserpuls is krachtig genoeg om fluorescente eiwitten kapot te maken (te bleken), zodat de FRAP-curve sterk daalt. De fluorescentie zal weer toenemen als de gebleekte eiwitten kunnen uitwisselen met andere, ongebleekte, eiwitten. Door analyse van FRAP-curves lieten we zien dat de dynamiek van paxillin en vinculin in focale adhesies verassend stabiel en vergelijkbaar was, in twee celtypes van verschillende diersoorten. Bijna de helft van de in focale adhesies gebonden paxillin en vinculin eiwitten was stabiel gebonden met bindingstijden die vergelijkbaar waren met de gemiddelde levensduur van FA's. Zyxin en VASP bonden veel dynamische aan focale adhesies. Daarnaast hebben we laten zien dat de bindingsdynamiek van FA-eiwitten verandert met de ligging en oriëntatie van een focale adhesie. In focale adhesies die dicht bij de rand van het gehechte celmembraan liggen waren paxillin, zyxin en VASP dynamischer gebonden en hadden zij grotere gebonden fracties dan in FA's





die verder dan deze rand liggen. Zyxin en VASP bonden ook dynamischer en hadden grotere gebonden fracties in focale adhesies die een loodrechte oriëntatie t.o.v. deze membraanrand hadden dan in focale adhesies die hier parallel aan lagen. De verhoogde dynamiek van een belangrijk structureel eiwit als paxillin, zoals voor focale adhesies dicht bij de membraanrand, zou de dynamiek van de complete focale adhesie kunnen vergroten, terwijl een grotere gebonden fractie van de direct aan actine bindende eiwitten zyxin en VASP potentieel de koppeling van actine aan de betreffende FA's versterkt.

In **hoofdstuk 3** werd een fotoconversie analysemethode gericht op het specifiek visualiseren van stabiel gebonden eiwitten binnen subcellulaire structuren en organellen ontwikkeld. Deze techniek werd toegepast om de grote stabiel gebonden fracties van paxillin en vinculin in focale adhesies verder te kunnen onderzoeken. Dit liet zien dat, ondanks dat paxillin en vinculin uniform verdeeld waren over focale adhesies, de stabiele gebonden paxillin en vinculin eiwitten kleine clusters vormden binnen focale adhesies. Deze clusters waren vele malen kleiner voor paxillin dan voor vinculin. Dit betekent dat de stabiel gebonden paxillin eiwitten sterker concentreerde, aangezien we in hoofdstuk 2 lieten zien dat de stabiel gebonden fracties van deze eiwitten vrijwel even groot zijn. De stabiel gebonden eiwitclusters bevonden zich bovendien significant vaker aan de helft van de focale adhesie die het verst van de rand van het gehechte membraan af ligt, de FA-kant waar ook de actinevezel binnenkomt. De effecten van FA oriëntatie en ligging t.o.v. de membraanrand op de stabiel gebonden eiwitclusters bleken subtieler dan op de bindingsdynamiek van FA-eiwitten, maar het oppervlak van de stabiel gebonden vinculin clusters was significant groter voor parallel georiënteerde FA's dicht bij de membraanrand dan voor parallelle FA's die hier verder vandaan lagen.

In **hoofdstuk 4** werd de distributie van de geselecteerde FA-eiwitten langs de lange as van focale adhesies bestudeerd door middel van de superresolutie techniek structured illumination microscopy. Aan het uiteinde van het FA complex dat het dichtst bij de rand van het gehechte celmembraan ligt ('head'), stak paxillin verder uit dan de drie andere eiwitten. Aan het tegenoverliggende FA-uiteinde ('tail') staken juist vinculin, zyxin en VASP uit, waarbij vinculin het verst uitstak. Wanneer cellen gestimuleerd werden met HGF werden de paxillin heads korter en de zyxin tails langer. Bovendien hadden focale adhesies bij een uitstulpend of terugtrekkend celmembraan langere paxillin heads dan focale adhesies bij een stilliggende membraanrand. Samen suggereert dit dat beweging de distributie van FA eiwitten langs de lange as van focale adhesies beïnvloedt.

Tenslotte werd in **hoofdstuk 5** de koppeling tussen focale adhesies en actine

in detail bestudeerd met een techniek waarbij fluorescentie microscopie en elektronen microscopie in één apparaat worden gecombineerd. Dit liet zien dat vrijwel alle focale adhesies in de elektronenmicroscopie plaatjes donkerder kleuren rond de aanhechtingsplaats van de actine vezel. Dit lokaal verhoogde contrast duidt op een hogere eiwitdichtheid, wellicht in combinatie met een toename van de eiwit fosforylatie. In bijna driekwart van de focale adhesies vormden deze gebieden van verhoogd contrast een gevorkte nanostructuur, waarbij de actinevezel de stam van de vork vormt en de focale adhesie gebieden met verhoogd contrast de vork.



## Scientific publications

- ✧ **Karin Legerstee**, Bart Geverts, Johan A. Slotman, Adriaan B. Houtsmuller, *Dynamics and distribution of paxillin, vinculin, zyxin and VASP depend on focal adhesion location and orientation*. Sci Rep 9, 10460, 2019
- ✧ **Karin Legerstee**, Tsion E. Abraham, Wiggert A. van Cappellen, Alex Nigg, Johan A. Slotman, Adriaan B. Houtsmuller, *Growth factor dependent changes in nanoscale architecture of focal adhesions* – submitted
- ✧ **Karin Legerstee**, Jason Sueters, Gert-Jan Kremers, Jacob P. Hoogenboom, Adriaan B. Houtsmuller, *Correlative light and electron microscopy reveals fork-shaped structures at actin entry sides of focal adhesions* - manuscript in preparation

# Curriculum vitae

## Personal details

Name: Karin Legerstee  
Date and place of birth: 21<sup>st</sup> August 1986, Utrecht

## Education

2012-2020

- ✧ *PhD position Department of Pathology, Erasmus MC, Rotterdam*
  - Promotor: Prof. dr. A.B. Houtsmuller
  - Copromotor: Dr. W.A. van Cappellen
  - Multimodal Microscopy of Focal Adhesions

2008-2011

- ✧ *Master's degree Biomedical sciences, Neuroscience and Cognition, Experimental and Clinical Neuroscience, Utrecht University*
  - Major Research Project  
Rudolf Magnus Institute, University Medical Centre (UMC) Utrecht  
The intracellular signalling cascade activated by RGMa-signalling through neogenin
  - Minor Research Project  
Department of Pharmacology, University of Cambridge  
Examining Carbachol signalling through Adenylyl Cyclase 2 using live single cell imaging
  - Master Thesis  
Rudolf Magnus Institute, University Medical Centre (UMC) Utrecht  
Cytoplasmic FMRP-interacting protein (Cyfip1) – A key player in the pathophysiology of the fragile X syndrome?
  - X-track honours programme, graduate school of Life Sciences, Utrecht University
  - Editor in the editorial board of the student-run Journal of Neuroscience and Cognition



2005-2008

✧ *Bachelor's degree Biomedical sciences, cum laude, Utrecht University*

Specialising in the fields of neuroscience, cellular biology and immunology

1998-2005

✧ *Context and Language Integrated Learning Programme, cum laude, Anna van Rijn College, Nieuwegein*

– vwo-diploma track Nature and Health

– International Baccalaureate (IB) Diploma Programme Certificate for the subject English A2 Higher Level (the highest IB certificate to be obtained by non-native speakers)

# PhD Portfolio

## Personal details

Name:	Karin Legerstee
Erasmus MC department:	Pathology
Research school:	Molmed
PhD-period:	2012-2020
Promotor(s):	Prof. dr. A.B. Houtsmuller and dr. W.A. van Cappellen
Supervisor:	Prof dr. A.B. Houtsmuller

## PhD training

### ✧ *Courses*

- Workshop on photoshop and Illustrator CS5  
2012
- Imaging life at the molecular level  
2012
- Course on Molecular Medicine  
2012
- Follow-up workshop on Indesign CS6  
2013
- OIC AMIE symposium  
2013
- Basic course on 'R'  
2014

### ✧ *Seminars and workshops*

- Annual molecular medicine day (poster)  
2012-2015
- Annual MGC day  
2013-2014



- Invadosome (presentation)  
2013
- MGC PhD-retreat (presentation)  
2014
- The Netherlands Society for Microscopy Annual Meeting (poster)  
2012-2016
- ✧ *International conferences*
  - EMBO spatial (Israel)  
2013
  - Labelling and Nanoscopy (Germany)  
2014
- ✧ *Teaching*
  - Supervision HBO student final Master project  
2015
  - Practicals OIC microscopy courses for master students  
2012-2015
  - Practicals OIC microscopy courses for PhD students  
2013-2015
  - Teachers assistant Java programming course  
2018

